Deflection Theory Analysis of Suspension Bridges

Untersuchungen über die Formänderungstheorie von Hängebrücken

Recherches sur la théorie de la flexion des ponts suspendus

Dr. S. O. Asplund, Örebro

Synopsis

To present a speedier and more accurate working method for the analysis of the action of vertical loads on suspension bridges is the object of this paper. The assumptions made and equations solved are primarily the same as in the ordinary form of the deflection theory, as developed or used by Ritter [1, 2]), Müller-Breslau [3]), Melan [4], Moissieff [6]), Steinman [7, 11]), Martin [8]), Timo-

---

[1]) Ritter, W., Versteifungsfachwerke bei Bogen- und Hängebrücken, Zeitschrift für Bauwesen, 1877, p. 189.

[2]) Ritter, W., Statische Berechnung der Versteifungsfachwerke der Hängebrücken, Schweizerische Bauzeitung, 1883, p. 6.

[3]) Müller-Breslau, Heinrich F. B., Theorie der durch einen Balken versteiften Kette, Zeitschrift des Architekten- und Ingenieur-Vereins zu Hannover, vol. 27, 1881, p. 58—79.

[4]) Melan, Joseph, Theorie der eisernen Bogenbrücken und der Hängebrücken, 2nd Ed., Berlin, 1888.

[5]) Godard, T., Récherches sur le calcul de la résistance de tabliers des ponts suspendus, Annales des Ponts et Chaussées, vol. 8, 1894, p. 105—189.

[6]) Johnson, J. B., C. W. Bryan and F. E. Turneaure, The Theory and Practice of Modern Framed Structures, 2nd vol., 9th Ed., John Wiley & Sons, New York, 1911, p. 276, and succeeding editions.

[7]) Melan, J. and D. B. Steinman, Theory of Arches and Suspension Bridges, Mc Graw-Hill Book Co., New York, 1913.

[8]) Martin, The Theory of the Stiffened Suspension Bridge, Engineering, 1927, vol. 123, p. 506 (editorial).

[9]) Timoshenko, S., The Stiffness of Suspension Bridges, A.S.C.E. Transactions, 1930, vol. 94, p. 377.

[10]) Krivocheine, G. G., La théorie exacte des ponts suspendus à trois travées, Report of the 2nd International Congress for Bridge and Structural Engineering, Vienna, 1929, p. 617.

[11]) Steinman, D. B., A Practical Treatise of Suspension Bridges, 2nd Ed., John Wiley and Sons, 1929.

SHENKO [9]), and others. Consequently all results exactly agree with their findings. Influence lines are employed in essentially the same manner as GODARD almost unnoticed introduced 1894 [5, 12, 14]).

In the present paper the approach to the solutions is from a somewhat different angle, resulting in more general formulas. The form of the solutions is also accomodated to suit *practical* computations in the best possible manner. Minor effects in actual suspension bridges, such as caused by cable extensions, are systematically segregated to correction terms. The influence functions are also constructed with the intent that one and the same set of tables may be used in the analysis of the largest possible class of bridges. Thus the tables here published are adequate for the design of almost all suspension bridges with simply supported uniform stiffening girders, that is for the great majority of all bridges hereto designed. Special constraint values are added, whereby the same set of tables may also be used in the computation of bridges with continuous uniform stiffening girders.

The angular deviations of the cable elements and the assumption of equal suspender forces in the evaluation of the horizontal force cause small errors that have previously not been generally recognized [10]) [12]). The angular deviations generally reduce critical live load moments in actual bridges by less than 10 %. These minor effects are accounted for in the equations and theoretical solutions below. Their numerical evaluation is obvious but not exemplified in order to save space [19]).

The necessary brevity of the theoretical parts of this paper may cause a non-mathematical reader some effort. Still, a practical designer need not neces-

---

[12]) RODE, HANS H., New Deflection Theory, Det Kgl. Norske Videnskabers Selskabs Skrifter, No. 3, 1930.

[13]) STEINMAN, D. B., A Generalized Theory for Suspension Bridges, A.S.C.E. Transactions, 1934, p. 1133.

[14]) BACHET, M., Le calcul des ponts suspendus munis de poutres de rigidité, Travaux, 1936, p. 218.

[15]) HARDESTY, SHORTRIDGE and HAROLD E. WESSMAN, Preliminary Design of Suspension Bridges, A.S.C.E. Transactions, 1939, p. 579.

[16]) STÜSSI, FRITZ and ERNST AMSTUTZ, Verbesserte Formänderungstheorie von Stabbogen und verankerten Hängebrücken, Schweiz. Bauzeitung, 1940, July 6.

[17]) KLÖPPEL, KURT and KUO-HAO LIE, Berechnung der Hängebrücken nach der Theorie II. Ordnung unter Berücksichtigung der Nachgiebigkeit der Hänger, Stahlbau 1941, p. 85.

[18]) ASPLUND, SVEN OLOF, On the Deflection Theory of Suspension Bridges, Swedish Academy for Engineering Sciences, Proceedings No. 184, 1945 (first published as dissertation, Upsala 1943).

[19]) ASPLUND, S. O., Influence Functions for the Angular Deviation Correction in Suspension Bridges, Third Congress Preliminary Publication, Int. Ass'n for Bridge and Structural Engineering, Liége, 1948, p. 415. — In a one-span bridge with flexibility c between 10 and 20 the angular deviation correction for maximum positive moments at $x = 0{,}2\ l$ is found to amount to −6 to −7 % of 64 f^2/l^2 times the moment as calculated by the classical deflection theory.

sarily grasp all details of the theoretical exposition. The extensive numerical examples have been elaborated with the aim of being self-explanatory for similar practical computations. They contain all necessary references to the equations and tables employed in actual design computations.

The theoretical part could have been made less mathematical — but at the loss of such generality that unquestionably promotes a better insight into the problem and that furnishes the clue to the treatment of non-uniform stiffening girders. It can also be made *more* mathematical and general [20]), but the writer considers that the form here used is most expedient for the present purpose.

Assumptions

1. All stresses in the bridge remain within the limits of proportionality.

2. The initial dead load w is carried by the cable without causing stress in the stiffening truss at normal temperature. If the bridge is erected in such a manner (for example with an upward bend of the truss) that the dead load causes certain stresses in the stiffening truss, account may be taken hereof by simply adding the initial stresses to those computed under the assumption 2.

3. The cables are assumed to be perfectly flexible.

4. In the ordinary forms of the deflection theory [2–9]), [11–17]) the magnitude of the *horizontal force* (not the other statical quantities, as deflections and moments) is determined under the assumption of equal pull in all suspenders. The small error caused by this approximation may be corrected by the application of *the suspender pull correction* explained in this paper.

5. The suspender forces instead of being treated as concentrated forces are considered as distributed loads in the same manner as if the distance between the suspenders were very small. In making this assumption it is obviously necessary afterwards to correct the resulting quantities by positive and negative moments, shears, etc. caused by the action of the stiffening truss as a continuous beam supported at the suspender connections.

6. When establishing the differential equation of the elastic line of the stiffening girder, the points of the cable are assumed to move along fixed verticals. — Actually the cable points and their verticals also move longitudinally along the bridge [12]), mainly as the effect of slight angular changes of the cable elements as the cable deforms. The error caused by assumption 6 may be corrected by the application of an "angular deviation correction load" touched upon below. This correction is generally small and on the safe side for bridges with simply supported stiffening trusses.

---

[20]) If the differential equation of the problem is solved by series expansions according to the orthogonal eigenfunctions of a homogeneous equation of the boundary problem, the angular deviation effect may be included in the homogeneous part of the equation and continuous bridges be treated directly by influence lines [18]). Both these circumstances are essential in the evaluation and use of model-determined influence functions [18]).

7. The suspenders are assumed to remain vertical during the deformation of the bridge. The small error caused by this assumption may be evaluated according to methods of STÜSSI AND AMSTUTZ[16]) and others.

8. The small effect (generally only a fraction of one per cent [6]), [11]), [17])) of the suspender elongation and the tower shortening under live load is neglected.

9. The horizontal component of the cable pull is assumed to be alike in all spans of the cable. — When fixed tower bases are used the horizontal force in the side spans will differ from that of the main span, but usually by small amounts if the towers are well designed. The modification of the Deflection Theory for this complication offers no fundamental difficulties and has been carried through by many authors, to whom the reader is referred. KLÖPPEL AND LIE [17]) in one specific instance find a decrease of moments in the stiffening truss of 0,2 % due to the fixing of the tower bases.

Equilibrium of Cable and Truss

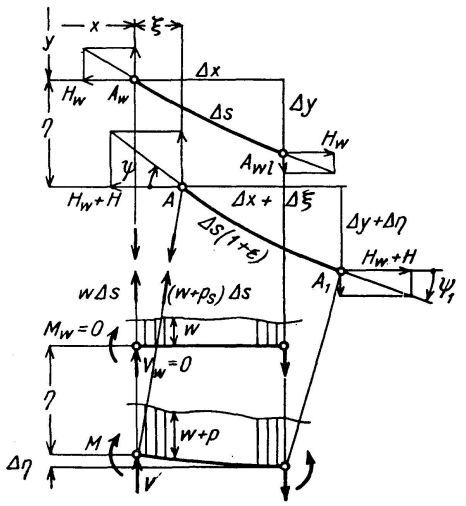

Fig. 1

In Fig. 1 $A_w(x,y) - A_{w1}(x+\Delta x, y+\Delta y)$ is a short piece Δs of the cable when the bridge is loaded by dead load w only. After the bridge is also loaded by live load p and is subjected to a change of temperature this piece of the cable has moved to $A(x+\xi,\ y+\eta) - A_1(x+\xi+\Delta x+\Delta\xi,\ y+\eta+\Delta y+\Delta\eta)$ and its length has increased to $\Delta s\,(1+\epsilon)$, $\epsilon\,\Delta s$ being the elastic and temperature elongation of $A_w A_{w1}$.

If A_{w1} approaches A_w,

$$(\Delta s)^2 = (\Delta x)^2 + (\Delta y)^2$$

and

$$(\Delta s)^2\,(1+\epsilon)^2 = (\Delta x + \Delta\xi)^2 + (\Delta y + \Delta\eta)^2$$

A short consideration of conditions in actual bridges reveals that at least ϵ^2 may be disregarded without practical error. Subtraction and division by the small quantity Δx yields

$$2\,s'^2\,\epsilon = 2\,\xi' + \xi'^2 + 2\,y'\,\eta' + \eta'^2$$

$$\xi' = -y'\,\eta' + s'^2\,\epsilon - \tfrac{1}{2}\,\eta'^2 - \tfrac{1}{2}\,\xi'^2$$

In the last term the main term $-y'\,\eta'$ may be substituted for ξ'

$$\xi' = -y'\,\eta' + s'^2\,\epsilon - \tfrac{1}{2}\,s'^2\,\eta'^2 \qquad (1)$$

Considering the coordinates $x + \xi$ and $y + \eta$ of the cable curve at A as functions of the parameter x, the direction of the tangent to the cable curve at A is given by

$$\tan \psi = \frac{d(y+\eta)}{dx} \Big/ \frac{d(x+\xi)}{dx} = \frac{y' + \eta'}{1 + \xi''} \tag{2}$$

and the direction of the tangent at A_1 by

$$\tan \psi_1 = \tan \psi + \frac{d \tan \psi}{dx} \Delta x + \dots$$

Using Assumption 7 the horizontal component of the cable pull increases to $H_w + H$, alike at A and A_1. In equilibrium the algrebraic sum of the vertical components at A and A_1 must equal the total suspender load $(w + p_s)\,\Delta x$ in the element Δx of the stiffening truss:

$$(H_w + H)(\tan \psi - \tan \psi_1) = (w + p_s)\,\Delta x \tag{3}$$

Retaining only $\xi' = - y' \eta'$ in (1) one may write $1/(1 + \xi') \approx l + \eta' y'$. Hence (3) and (2) give

$$- \frac{w + p_s}{H_w + H} = (\tan \psi)' = \left(\frac{y' + \eta'}{1 + \xi'} \right)' \approx y'' + \eta'' + (y' \cdot \eta' y')' \tag{4}$$

since η' may be dropped at the side of y' in the small last term.

The stiffening girder carries the load $p_l = p - p_s$, p being the live load on the bridge and p_s the suspender pull caused by it. The common theory of beams asserts that the negative second derivative of the truss or girder moment $- E I \eta''$ is equal to the load carried by the girder:

$$p_l = -(- E I \eta'')'' = p - p_s - w + w = p + (H_w + H)[y'' + \eta'' + (y'^2 \eta')'] - H_w y''$$

$$(E I \eta'')'' - (H_w + H)\eta'' = H y'' + p + (H_w + H)(y'^2 \eta')'$$

$$= H y'' + P(x) = \Phi(x) \tag{5}$$

remembering that the dead load of the bridge $w(x) = - H_w y''$, cf. (4) for p, p_s, H, ξ, and $\eta = 0$. The term $(H_w + H)(y'^2 \eta')'$ is referred to as the (angular deviation) *correction load*. It is generally small and may be omitted in all calculations of ordinary accuracy. In any case it can be taken care of by iteration. The correction load causes "angular deviation corrections" in deflections, moments, etc. These corrections may be evaluated separately by influence functions [19]).

The "fundamental equation" (5) could properly be attributed to Rode [12]), who first established this equation, although in slightly less general form. Its last term is the correction term for the angular deviations just mentioned of the cable elements, cf. Assumption 6. If that term is omitted (5) becomes

Melan's equation [4, 21]), which is commonly used in the deflection theory of suspension bridges. The correction term may be combined with the second term on the left side:

$$(E\,I\,\eta'')'' - (H_w + H)\,[(1 + y'^2)\,\eta']' = Hy'' + p \tag{6}$$

If $H_w + H$ is treated as a constant and the right hand side as a function of x only, (5) or (6) may be recognized as a self-adjoint linear differential equation of the fourth order. Its solution is restricted by linear boundary conditions: the cable condition and the support and continuity conditions for the stiffening truss.

The Cable Condition

Both sides of (1) are integrated over all cable parts C that are elastically affected by the cable tension

$$\int_c \xi'\,dx = -\int_c y'\,\eta'\,dx + \int_c s'^2\,\epsilon\,dx - \tfrac{1}{2}\int_c s'^2\,\eta'^2\,dx$$

$\int_c \xi'\,dx = \int_c d\xi$ obviously represents the increase ΔL in the horizontal distance L between the cable anchorage points.

The effect of temperature is generally treated as an elongation $\epsilon = \omega t$ of the cable only, ω being the coefficient of thermal expansion and t the *rise* in temperature. This yields an integral term $\omega t \int_c s'^2\,dx$ in the above equation. But also the towers and the suspenders are elongated by a rise in temperature. While this in general complicates the solution, it is simplified if the whole structure *above* the straight line connecting both anchorage points is regarded as subjected to the rise in temperature. This assumption [22]) better conforms to actual conditions than if only the cable elongates. It also results in simpler and easier formulas, since the effect of a rise in temperature simply becomes equivalent to a decrease of $\omega t L$ in the distance between the anchorages.

When the influence of thermal elongation has now been taken care of in the left side of the equation, only the elastic elongation $Hs'/E_c A_c$ will remain for ϵ. Partial integration of $-\int_c y'\,\eta'\,dx$ yields $-[y'\,\eta]_c + \int_c y''\,\eta\,dx$ where the first term is zero, since $\eta = 0$ at the anchorages. Removing the last term to the left hand side and all the other terms, the "cable yield", to the right hand side, the cable condition becomes

$$\int_c y'\,\eta'\,dx = -\int_c y''\,\eta\,dx = \beta\gamma\,L_s + \omega t\,L - \Delta L - \tfrac{1}{2}\int_c (s'\,\eta')^2\,dx = \Delta C \tag{7}$$

where

$$\beta = \frac{H}{H_w} \tag{8}$$

---

[21]) "Melan's equation" was first established and solved by W. RITTER[2]) and MÜLLER-BRESLAU[3]).

[22]) By J. M. FRANKLAND, see [13]), p. 1203.

and the "cable factor"

$$\gamma = \frac{H_w}{E_c A_{c0}} \tag{9}$$

and the "elastic length" of the cable

$$L_s = \int_C \frac{E_c A_{c0}}{E_c A_c} s'^3 \, dx \tag{10}$$

A_{c0} denotes any suitable mean area of the cable.

An approximate expression for a constant cable section area $A_c = A_{c0}$ and constant dead load w in each span is

$$L_s = \Sigma l_\nu \sec^3 \alpha_\nu (1 + 8 f_\nu^2 / l_\nu^2) \tag{11}$$

where α_ν is the slope of the cable chord in the νth span. The sum should be extended over all spans ν of the *cable* [23]).

The term $-\frac{1}{2}\int (s'\eta')^2 dx$ of (7) corrects the approximation made by Assumption 4 and therefore may be termed the suspender pull correction [24]).

General solution of the fundamental equation

The live load horizontal force H or β is a function (7) of η. This makes the fundamental equation (5) or (6) very complicated and insolvable by known functions or finite methods. If, however, the variable H is treated as a constant, the equation together with its boundary conditions, the support conditions and the cable condition, may be recognized as a self-adjoint linear boundary problem of the fourth order with variable coefficients in the differential equation. Accordingly, one enters a plausible value of H in the fundamental equation. From its solution η, a value of β or H is calculated according to (7). This value is again entered in the fundamental equation. By iteration of the solution with successively corrected values of H the exact solution of the fundamental equation and its boundary conditions may be approached to any desired accuracy. In practical bridge problems the convergence of this process is rapid. More than one or two iterations are seldom required.

The solution of the fourth order linear boundary problem may be effectuated by series expansions of orthogonal eigenfunctions or, a little less general, by the theory of Green functions in the following manner.

---

[23]) Previously, the expressions $L_s = \Sigma l_\nu (\sec^3 \alpha_\nu + 8 f_\nu^2 / l_\nu^2)$ and $L_s = \Sigma l_\nu (\sec^3 \alpha_\nu + 8 \sec \alpha_\nu f_\nu^2 / l_\nu^2)$ have been used. The reader may verify that (11) is better, since it includes more terms from the expansion of s'^3 in $\int s'^3 dx$.

[24]) KRIVOCHEINE[10]) gives the slightly less accurate correction $-\frac{1}{2}\int \eta\eta'' dx$.

In an interval $a \leqq x \leqq b$ in which $p(x)$ is continuous the general solution of the linear differential equation

$$y'' + p(x)\,y = f(x) \tag{12}$$

with the boundary conditions $y(a) = y(b) = 0$ may be written

$$y = \frac{y_2(x)}{W}\int_a^x y_1(k)\,f(k)\,dk + \frac{y_1(x)}{W}\int_x^b y_2(k)\,f(k)\,dk + C_1 y_1(x) + C_2 y_2(x) \tag{13}$$

Here y_1 and y_2 are linearly independent particular solutions of the associated homogeneous equation $y'' + py = 0$. Then the constant Wronskian $W = y_1 y'_2 - y_2 y'_1$ becomes $\neq 0$. If y_1 and y_2 are determined in such a manner that $y_1(a) = y_2(b) = 0$ one obtains $C_1 = C_2 = 0$ in (2).

These theorems are easily proved by differentiation twice of (13) and substitution in (12).

Introducing the moment M in the truss, (5) may now be split in two equations

$$\eta'' = -\frac{M}{EI(x)} \tag{14}$$

$$M'' - \frac{H_w + H}{EI}M = -\Phi(x) \tag{15}$$

Assuming that the stiffening girder of the nth span is simply supported at its ends $x = 0$ and $x = l_n$ hence $\eta(0) = \eta(l_n)$ and $M(0) = M(l_n) = 0$, assuming that two linearly independent particular integrals $M_1(x)$ and $M_2(x)$, $M_1(0) = 0$, $M_2(l_n) = 0$, have been found of the associated homogeneous equation to (4)

$$M'' - \frac{H_w + H}{EI}M = 0 \tag{16}$$

and forming the Green function

$$\left.\begin{aligned} K(x,k) &= \frac{1}{W}M_1(x)\,M_2(k) \quad \text{for } x \leqq k \\ &= \frac{1}{W}M_2(x)\,M_1(k) \quad \text{for } x \geqq k \end{aligned}\right\} \tag{17}$$

with $W = M_1 M'_2 - M_2 M'_1$, the general solution of (15) is by (13)

$$M(x) = -\int_o^{l_n} K(x,k)\,\Phi(k)\,dk$$

Now $M(x)$ is a known function by which η may be similarly determined from (14). The associated homogeneous equation $\eta''(x) = 0$ is satisfied by the two linearly independent solutions $\eta_1 = x$ and $\eta_2 = l_n - x$, which also satisfy

the boundary conditions $\eta_2(0) = \eta_2(l_n) = 0$. The normalizing condition is $W_1 = \eta_1 \eta_2' - \eta_2 \eta_1' = -l_n$. Writing

$$\left.\begin{aligned} K_1(x,t) &= -\frac{1}{l_n} x(l_n - t) \quad \text{for} \quad x \leqq t \\ &= -\frac{1}{l_n}(l_n - x)\, t \quad \text{for} \quad x \geqq t \end{aligned}\right\}$$

(13) will again furnish the solutions of (14):

$$\eta(x) = -\int_0^{l_n} K_2(x,t) \frac{M}{EI(t)}\, dt = \frac{1}{H_w + H} \int_0^{l_n} J_{xk}\, \Phi(k)\, dk \tag{18}$$

where

$$\frac{1}{H_w + H} J_{xk} = \int_0^{l_n} \frac{1}{EI(t)} K_1(x,t)\, K(t,k)\, dt$$

By a short deduction, subdividing the integration interval into three parts (0 to x, x to k and k to l_n for $x \leqq k$), this integral is found to be

$$\left.\begin{aligned} J_{xk} &= \frac{1}{l_n} x(l_n - k) + \frac{1}{W} M_1(x)\, M_2(k) \quad \text{for} \quad x \leqq k \\ &= \frac{1}{l_n}(l_n - x)\, k + \frac{1}{W} M_2(x)\, M_1(k) \quad \text{for} \quad x \geqq k \end{aligned}\right\} \tag{19}$$

Noting by (4) that $H_w y''(x) = -w(x)$, (18) becomes

$$\eta(x) = \frac{1}{H_w + H}\left[\int_0^{l_n} J_{xk}\, P(k)\, dk - \beta J_x\right] \tag{20}$$

with

$$J_x = \int_0^{l_n} J_{xk}\, w(k)\, dk \tag{21}$$

Now (20) is entered into the cable condition (7)

$$-\int_S -\frac{w(x)}{H_w} \frac{1}{H_w + H}\left[\int_0^{l_n} J_{xk}\, P(k)\, dk - \beta J_x\right] d\dot{x} = \Delta C$$

The first integral must be extended over *all* spans $= 1,2 \ldots N$ suspended from the cable. Using (21) one obtains

$$\int_C J_k\, P(k)\, dk - \beta \sum_{\nu=1}^{N} \int_0^{l_\nu} w(x)\, J_x\, dx = H_w (H_w + H)\, \Delta C$$

Abbreviating

$$G = \sum_{\nu=1}^{N} \int_0^{l_\nu} w(x)\, J_x\, dx \tag{22}$$

with the sum extended from $\nu = 1$ to $\nu = N$ (including all spans suspended from the cable), and, see (7),

$$\delta = (1 + \beta)\, \frac{H_w^2}{G}\, \Delta C \tag{23}$$

one obtains

$$\beta = \int_S \frac{J_k}{G}\, P(k)\, dk - \delta \tag{24}$$

Remembering that $J_{xk} = 0$ in all spans except the nth (that of the section x), (20) may be written

$$\eta = \frac{1}{H_w + H} \left[\sum_{\nu=1}^{N} \int_0^{l_n} \left(J_{xk} - J_x \frac{J_k}{G} \right) P(k)\, dk + \delta J_x \right]$$

Denote

$$I_{xk}^{(i)} = J_{xk}^{(i)} - J_x^{(i)} \frac{J_k}{G}$$

$$\left.\begin{aligned} J_x^{\mathrm{I}} &= \frac{dJ}{dx}, \quad J_x^{\mathrm{II}} = -\frac{EI(x)}{H_w + H} \frac{dJ_x}{dx}, \quad J_x^{\mathrm{III}} = \frac{dJ_x^{\mathrm{II}}}{dx}, \quad J_x^{\mathrm{IV}} = \frac{dJ_x^{\mathrm{III}}}{dx} \\ J_{xk}^{\mathrm{I}} &= \frac{\partial J_{xk}}{\partial x}, \quad J_{xk}^{\mathrm{II}} = -\frac{EI(x)}{H_w + H} \frac{\partial J_{xk}^{\mathrm{I}}}{\partial x}, \quad J_{xk}^{\mathrm{III}} = \frac{\partial J_{xk}^{\mathrm{II}}}{\partial x}, \quad J_{xk}^{\mathrm{IV}} = \frac{\partial J_{xk}^{\mathrm{III}}}{\partial x} + e_{xk} \end{aligned}\right\} \tag{25}$$

where e_{xk} has the value $1/2\epsilon$ between $k = x - \epsilon$ and $x + \epsilon$, $\epsilon \to 0$, and is otherwise zero. We finally obtain

$$\left.\begin{aligned} \eta &= \frac{1}{H_w + H} \left[\int_S I_{xk}\, P(k)\, dk + \delta J_x \right] \\ \eta' &= \frac{1}{H_w + H} \left[\int_S I_{xk}^{\mathrm{I}}\, P(k)\, dk + \delta J_x^{\mathrm{I}} \right] \\ M &= \int_S I_{xk}^{\mathrm{II}}\, P(k)\, dk + \delta J_x^{\mathrm{II}} \\ V &= \int_S I_{xk}^{\mathrm{III}}\, P(k)\, dk + \delta J_x^{\mathrm{III}} \\ p_s = p - p_t &= \int_S I_{xk}^{\mathrm{IV}}\, P(k)\, dk + J_x^{\mathrm{IV}} \end{aligned}\right\} \tag{26}$$

for $$-p_t = \frac{\partial V}{\partial x} \quad \text{and} \quad \int_{k=x+\epsilon}^{x-\epsilon} e_{xk}\, P(k)\, dk = \frac{1}{2\epsilon} p(k)\, 2\epsilon = p(k).$$

Identical influence line expressions (26) are obtained also for the more general case of continuous stiffening girders. This may be proved by an expansion of the solution of the boundary problem according to the characteristic (orthogonal) functions of the homogeneous fundamental differential equation associated to (6)[25]). If so desired the correction load term can at the same time be retained in the homogeneous part of the equation. This is made use of in the case of model-determined influence functions[26]).

Influence Functions Developed

Denoting for temporary abbreviation $X = x/l_n$ and $K = k/l_n$ (19) and (25) yield for the calculation of $J_{xk}^{(i)}$ and $J_x^{(i)}$ the following values in the nth span:

(27)

functions $j_{xk}^{(i)}$	$k_n \leqq x_n$	$k_n \geqq x_n$
$j_{xk} = \frac{1}{l_n} J_{xk} =$	$\frac{1}{l_n W} M_2(x)\, M_1(k) + (1-X)\, K$	$\frac{1}{l_n W} M_1(x)\, M_2(k) + X(1-K)$
$j_{xk}^{\mathrm{I}} = J_{xk}^{\mathrm{I}} =$	$\frac{1}{W} M_2'(x)\, M_1(k) - K$	$\frac{1}{W} M_1'(x)\, M_2(k) + 1 - K$
$j_{xk}^{\mathrm{II}} = \frac{1}{l_n} J_{xk}^{\mathrm{II}} =$	$-\frac{1}{l_n W} M_2(x)\, M_1(k)$	$-\frac{1}{l_n W} M_1(x)\, M_2(k)$
$j_{xk}^{\mathrm{III}} = J_{xk}^{\mathrm{III}} =$	$-\frac{1}{W} M_2'(x)\, M_1(k)$	$-\frac{1}{W} M_1'(x)\, M_2(k)$
$j_{xk}^{\mathrm{IV}} = l_n J_{xk}^{\mathrm{IV}} =$	$-\frac{H_w + H}{EI} \frac{l_n}{W} M_2(x)\, M_1(k)$	$-\frac{H_w + H}{EI} \frac{l_n}{W} M_1(x)\, M_2(k)$
$j_{xk}^{\mathrm{II}} =$	$\frac{EI}{H_w + H} \frac{1}{l_n^2} j_{xk}^{\mathrm{IV}}$	$\frac{EI}{H_w + H} \frac{1}{l_n^2} j_{xk}^{\mathrm{IV}}$
$j_{xk}^{\mathrm{I}} =$	$- j_{xk}^{\mathrm{III}} - K$	$- j_{xk}^{\mathrm{III}} + 1 - K$
$j_{xk} =$	$- j_{xk}^{\mathrm{II}} + (1 - X)\, K$	$- j_{xk}^{\mathrm{II}} + X(1-K)$

and functions $j_x^{(i)}$ (28)

$$j_x = \frac{1}{w_n l_n^2} J_x = \int_0^1 j_{xk} \frac{w(k)}{w_n} dK = (1-X) \int_0^x K \frac{w(k)}{w_n} dK + X \int_x^1 (1-K) \frac{w}{w_n} dK +$$

[25]) See [18]), p. 31—37. Rudberg, see [18]), p. 170, later outlined the solution by Green functions of the equation $[I(x)\eta'']'' - K^2\eta'' = F(x)$ with the conditions $\eta = \eta'' = 0$ at $x = 0$ and l (no cable condition).

[26]) See [18]), p. 110—137.

$$+\frac{M_2(x)}{l_n W}\int_0^x M_1(k)\frac{w}{w_n}dK+\frac{M_1(x)}{l_n W}\int_x^1 M_2(k)\frac{w}{w_n}dK$$

$$j_x^{\mathrm{I}}=\frac{1}{w_n l_n}J_x^{\mathrm{I}}=+\frac{M_2'(x)}{W}\int_0^x M_1(k)\frac{w}{w_n}dK+\frac{M_1'(x)}{W}\int_x^1 M_2(k)\frac{w}{w_n}dK-$$

$$-\int_0^x K\frac{w}{w_n}dK+\int_x^1(1-K)\frac{w}{w_n}dK$$

$$j_x^{\mathrm{II}}=\frac{1}{w_n l_n^2}J_x^{\mathrm{II}}=-\frac{M_2(x)}{l_n W}\int_0^x M_1(k)\frac{w}{w_n}dK-\frac{M_1(x)}{l_n W}\int_x^1 M_2(k)\frac{w}{w_n}dK$$

$$j_x^{\mathrm{III}}=\frac{1}{w_n l_n}J_x^{\mathrm{III}}=-\frac{M_2'(x)}{W}\int_0^x M_1(k)\frac{w}{w_n}dK-\frac{M_1'(x)}{W}\int_x^1 M_2(k)\frac{w}{w_n}dK$$

$$j_x^{\mathrm{IV}}=\frac{1}{w_n}J_x^{\mathrm{IV}}=-\frac{c_n^2}{i_n}\frac{M_2(x)}{l_n W}\int_0^x M_1(k)\frac{w}{w_n}dK-\frac{c_n^2}{i_n}\frac{M_1(x)}{l_n W}\int_x^1 M_2(k)\frac{w}{w_n}dK-\frac{w(x)}{w_n}$$

$$j_x^{\mathrm{II}}=\frac{EI}{H_w+H}\frac{1}{l_n^2}\left[j_x^{\mathrm{IV}}+\frac{w(x)}{w_n}\right]$$

$$j_x^{\mathrm{I}}=-j_x^{\mathrm{III}}-\int_0^x K\frac{w}{w_n}dK+\int_x^1(1-K)\frac{w}{w_n}dK$$

$$j_x=-j_x^{\mathrm{II}}+(1-X)\int_0^x K\frac{w(k)}{w_n}dK+X\int_x^1(1-K)\frac{w}{w_n}dK$$

Here w_n denotes a suitable mean value of the dead load $w(k)$ in the nth span. The property of M_1 and M_2 to satisfy (16) is used.

The fourth equations of (27) show that there is an increase of

$$-\frac{1}{W}M_1'(x)M_2(x)+\frac{1}{W}M'_2(x)\,M_1(x)=1$$

in the functions j_{xk}^{III} and J_{xk}^{III} as k passes from $x-0$ to $x+0$, and as x passes from $k-0$ to $k+0$ there is a decrease of 1. The derivative $\frac{\partial J_{xk}^{\mathrm{III}}}{\partial x}$ therefore has the value $-e_{xk}$ at $x=k$. This distinct infinite influence ordinate is exactly nullified in the definition in (25) of J_{kx}^{IV} and in the definition in (27) of j_{xk}^{IV}.

If further

$$g_\nu=\int_0^1\frac{w(x)}{w_\nu}j_x\,d\frac{x}{l_\nu},\quad G_\nu=w_\nu^2 l_\nu^3 g_\nu \tag{29}$$

(22) gives

$$G=\sum_{\nu=1}^{N}G_\nu \tag{30}$$

and if one writes

$$\beta_\nu = \int_0^{l_\nu} \frac{J_k}{G_\nu} P(k)\, dk = \int_0^1 \frac{j_k}{g_\nu} \frac{P(k)}{w_\nu} d.\frac{k}{l_\nu} \tag{31}$$

(24) gives

$$\beta = \frac{1}{G} \sum_{\nu=1}^{N} w_\nu^2\, l_\nu^3\, g_\nu \beta_\nu - \delta = \Sigma \frac{G_\nu}{G} \beta_\nu - \delta \tag{32}$$

The Precise Determination of the Critical Load Position

These solutions have been established with the aim of referring all effects of cable elongations to correction terms, the δ-terms of (26). This offers a great advantage since all influence functions may be computed entirely independent of the cables. For a given position of the live loading this method will yield exact results. However, the zero-point of the influence line may be somewhat displaced and cause some error in the establishment the critical *position* of the live load. To ascertain the correct critical position the influence line may be corrected near the zero-point [27]).

Equations (7), (23), and (24) yield

$$\delta = \frac{H_w (H_w + H)}{G} \left[\gamma L_s \left(\int \frac{J_k}{G} P(k)\, dk - \delta \right) + \omega t L - \Delta L - \tfrac{1}{2} \int_C (s'\eta')^2\, dx \right]$$

$$\delta = T \int_C \frac{J_k}{G} F(k)\, dk + \delta_0, \quad T = \frac{U}{1+U}, \quad U = (1+\beta) \frac{H_w^2}{G} \gamma L_s \tag{33}$$

$$\delta_0 = \frac{T}{\gamma L_s} \left[\omega t L - \Delta L - \tfrac{1}{2} \int_C (s'\eta')^2\, dx \right] \tag{34}$$

Thus for instance the third equation (26) may be written

$$M = \int \left(I_{xk}^{II} + T J_x^{II} \frac{J_k}{G} \right) P(k)\, dk + \delta_0 J_x^{II}$$

that is, *the influence line* I_{xk}^{II} *should be corrected with the influence line for horizontal force* J_k/G *times* $T J_x^{II}$ . . . . . (35)

However, such exactitude in the establishment of the critical load *position* is seldom required (only for very meticulous computations of stiff bridges). Then it may be confined to the correction of only one or two ordinates near the zero-points.

---

[27]) By BERGFELT, see [18]), p. 148.

Computation of influence functions for multiple-span bridges from those for one-span bridges

The influence functions for bridges with several simply supported spans may be computed from those of one-span bridges according to the following formulas (36) and (37). The first equation (25) may be written [28])

$$I_{xk}^{(i)} = I_{xkn}^{(i)} + J_x^{(i)} \frac{J_k}{G_n}\left(1 - \frac{G_n}{G}\right), \quad I_{xkn}^{(i)} = J_{xk}^{(i)} - J_x^{(i)} \frac{J_k}{G_n} \tag{36}$$

Obviously $I_{xkn}^{(i)}$ here denote the influence functions of the span n of the section x when that span is the span of a one-span bridge. The expression (36) for the influence functions $I_{xk}^{(i)}$ may be suitably used for the span n of the section x. According to (19) or (27) $J_{xk}^{(i)}$ is zero when the load k is in other spans m than that of the section x. For these other spans (25) may be written

$$I_{xk}^{(i)} = -\frac{G_m}{G} J_x^{(i)} \frac{J_k}{G_m} \qquad (m \neq \text{span of } x) \tag{37}$$

Analysis of multiple-span bridges with direct use of the influence functions for one-span bridges

However, in the analysis of multiple span bridges with simply supported spans it is feasible and very often expedient to refer to the δ-terms also the effects of live loads applied to other spans than that of the section x [29]). Entering (36) and (37) in for instance the first equation (26) and using (31) results in

$$\eta = \frac{1}{H_w + H}\left[\int_0^{l_n} I_{xkn}\, P(k)\, dk + J_x \beta_n - J_x \frac{1}{G} \Sigma G_\nu \beta_\nu + \delta J_x\right] =$$

$$= \frac{1}{H_w + H}\left[\int_0^{l_n} I_{xkn}\, P(k)\, dk + \delta_n J_x\right]$$

where the sum should be extended over all spans and

$$\delta_n = \beta_n - \frac{1}{G} \Sigma G_\nu \beta_\nu + \delta = \beta_n - \beta \tag{38}$$

Thus all equations (26) *still are valid if* δ *is replaced by* δ_n *according to* (38), $I_{xk}^{(i)}$ *by* $I_{xkn}^{(i)}$, *and the integrals extended only over the span* l_n *of the section* x *considered* . . . . . (39)

---

[28]) SELBERG, see [18]), p. 150, first indicated an analogous procedure for spans of even stiffness.

[29]) HARDESTY and WESSMAN, see [14]), p. 579, also treat such "span-interaction" separately.

The integral of (24) used in the determination of H and δ_n, must still be extended over all spans.

The accuracy of the results of this computation is not influenced for a live load of a predetermined position, but in the determination of the critical live load *position* an error may enter. To avoid such errors in the critical live load position, the influence line $I^{(i)}_{xkn}$ may be corrected near its zero-points. Applying (33), (36), and (37) to (26) one finds for instance

$$(H_w + H)\,\eta = \int_0^{l_n} \left[I_{xkn} + J_x \frac{J_k}{G_n} - J_x (1 - T) \frac{G_n}{G} \frac{J_k}{G_n} \right] P(k)\, dk - \\ - \sum_{\neq n} \int_0^{l_m} J_x (1 - T) \frac{G_m}{G} \frac{J_k}{G_m} P(k)\, dk + \delta_0 J_x$$

where the sum should be extended over all spans except that of the section x considered.

This indicates that *the influence line $I^{(i)}_{xkn}$ in the span of the section x should be corrected by the influence line for the single-span horizontal force J_k/G_n times $J^{(i)}_x\,[1 - (1 - T)\,G_n/G]$ and that instead of the zero influence lines of other spans m the respective horizontal force influence lines J_k/G_m times $- J^{(i)}_x (1 - T)\,G_m/G$ should be considered* . . . . . (40)

These precautions in the determination of the live load position need not generally be *numerically* completed other than for *one* value near the zero-point(s) of $I^{(i)}_{xkn}$. With the notation, compare (36),

$$i^{(i)}_{xkn} = i^{(i)}_{xk} = j^{(i)}_{xk} - j^{(i)}_x \frac{j_k}{g_n} \tag{41}$$

the formulas (26) may be rewritten by (39), (36), (27), (28), and (29) in the following form

$$\left.\begin{aligned} \frac{\eta}{l_n} &= \frac{w_n l_n}{H_w} \frac{1}{1+\beta} \left[\int_0^1 i_{xk} \frac{P(k)}{w_n} d\frac{k}{l_n} + \delta_n j_x \right. \\ \eta' &= \frac{w_n l_n}{H_w} \frac{1}{1+\beta} \left[\int_0^1 i^{\mathrm{I}}_{xk} \frac{P(k)}{w_n} d\frac{k}{l_n} + \delta_n j^{\mathrm{I}}_x \right] \\ \frac{M}{w_n l_n^2} &= \int_0^1 i^{\mathrm{II}}_{xk} \frac{P(k)}{w_n} d\frac{k}{l_n} + \delta_n j^{\mathrm{II}}_x \\ \frac{V}{w_n l_n} &= \int_0^1 i^{\mathrm{III}}_{xk} \frac{P(k)}{w_n} d\frac{k}{l_n} + \delta_n j^{\mathrm{III}}_x \\ \frac{p_s}{w_n} &= \int_0^1 i^{\mathrm{IV}}_{xk} \frac{P(k)}{w_n} d\frac{k}{l_n} + \delta_n j^{\mathrm{IV}}_x \end{aligned}\right\} \tag{42}$$

the integrals being extended over the span n only of the section x considered. These formulas together with (32) for the horizontal force increment and (38) for δ_n may be suitably used in calculations according to this article.

In the accurate establishment of the critical live load position *the influence functions* $i_{xk}^{(i)}$ *in the span n of the section x should be corrected by the influence functions for the single span horizontal force* j_k/g_n *times* $j_x^{(i)}\,[1-(1-T)\,G_n/G]$, *and the* $i_{xkn}^{(i)} = 0$ *influence functions of the other spans m by their respective horizontal force influence functions* j_k/g_m *times* $-j_x^{(i)}\,(1-T)\,G_m/G$ . . . . . (43)

(In using thus corrected influence lines for the complete analysis the δ_n-terms of (42) vanish, but one contribution to η, η', etc, is obtained for each span. These contributions must be added.)

Tables for Uniform Stiffening Girders

All previous formulas are valid for variable stiffnesses $E\,I$. The influence functions $I_{xk}^{(i)}$ are functions of the variable coefficient $(H_w' + H)/E\,I$ of the homogeneous equation (16) and may, if evaluated, be tabulated in groups, each encompassing all spans of the same relative stiffness variation.

For uniform stiffness in a span n, $E\,I_n = \text{const.}$, it is expedient to introduce the notions of the *proper* flexibility c_{n0} and the *incidental* flexibility c_n of that span, defined by

$$c_{n0} = \sqrt{\frac{H_w\,l_n^2}{E\,I_n}}, \qquad c_n = \sqrt{\frac{(H_w+H)\,l_n^2}{E\,I_n}} = c_{n0}\,(1+\beta) \tag{44}$$

Particular integrals M_1 and M_2 of (16), $M'' - M c_n^2/l_n^2 = 0$, satisfying the boundary conditions $M_1(0) = 0$, $M_2(l_n) = 0$ are obviously

$$M_1 = \sinh c_n \frac{x}{l_n}, \qquad M_2 = \sinh c_n \left(1 - \frac{x}{l_n}\right)$$

hence

$$W = -\frac{c_n}{l_n} \sinh c$$

From these equations, the assumption of constant dead load in each span, the lowest five formulas in each group (27) and (28), the first formula (29), and from (41), the needed functions j_k/g_n, g_n, $j_x^{(i)}$, $i_{xk}^{(i)}$ and their end slopes $\dfrac{\partial j_{xk}^{(i)}}{\partial k/l_n}$ (see below under Continuous Stiffening Girders), have been numerically evaluated in the following tables[30]). Table 12 gives the positive and negative areas of the influence diagrams $i_{xk}^{(i)}$ and the simultaneous areas of the j_k/g-diagram.

[30]) The writer has computed such tables for $x/l = 0$, 0,1, 0,15, 0,20, 0,30, 0,40 and 0,50 [18]). However, for the present purpose it seems superfluous to publish other values than those of Tables 1 to 11, since the maximum moment and maximum deflection in most practical cases occur very close to $x = 0{,}2\,l$, the maximum shear at the supports and the maximum hanger reaction at mid-span.

Table 1. Values of j_k/g_n and of g_n

The three rows of $c = \infty$ should be added

c	j_k/g_n						$10^3\, g_n$
	End slope	$\frac{k}{l}=0{,}1$	0,2	0,3	0,4	0,5	
0	5,000	0,4905	0,9280	1,2705	1,4880	1,5625	$10^3c^2/120$
1	5,006	0,4909	0,9285	1,2704	1,4876	1,5619	7,57
2	5,021	0,4922	0,9295	1,2703	1,4860	1,5597	23,73
3	5,049	0,4943	0,9315	1,2702	1,4836	1,5564	39,27
4	5,082	0,4968	0,9337	1,2700	1,4808	1,5524	50,96
5	5,120	0,4997	0,9361	1,2697	1,4776	1,5481	59,12
6	5,159	0,5026	0,9387	1,2694	1,4744	1,5437	64,77
7	5,199	0,5056	0,9411	1,2690	1,4712	1,5395	68,75
8	5,238	0,5084	0,9433	1,2686	1,4682	1,5353	71,61
10	5,310	0,5134	0,9471	1,2677	1,4628	1,5282	75,33
12	5,373	0,5177	0,9502	1,2670	1,4587	1,5228	77,55
15	5,455	0,5227	0,9534	1,2658	1,4540	1,5169	79,48
20	5,550	0,5283	0,9564	1,2643	1,4492	1,5108	81,08
40	5,743	0,5365	0,9593	1,2615	1,4428	1,5032	82,74
∞	6,000	0,5400	0,9600	1,2600	1,4400	1,5000	83,33
	$-12/c$						
	$+72/c^2$	$-5{,}52/c^2$	$-0{,}48/c^2$	$+3{,}12/c^2$	$+5{,}28/c^2$	$+6{,}00/c^2$	$-1/c^2$

Table 2. Values of $10^3\, j_x^{(i)}$

$j_x''' = 0$ for $x_n = 0{,}5\, l_n$ and all c_n.

c	$10^3\, j_x$		$10^3\, j_x^{\mathrm{I}}$	$10^3 j_x^{\mathrm{II}}$		$10^3\, j_x^{\mathrm{III}}$	$10^3\, j_x^{\mathrm{IV}}$	
	$\frac{x}{l}=0{,}2$	0,5	0	0,2	0,5	0	0,2	0,5
$\to 0$	$7{,}73c^2$	$13{,}0c^2$	$41{,}7c^2$	80,00	125,00	500,0	1000	1000
1	7,03	11,82	37,88	72,97	113,18	462,1	972,0	886,8
2	22,06	37,01	119,2	57,94	87,99	380,8	768,3	648,1
3	36,58	61,12	198,3	43,42	63,88	301,7	609,2	425,1
4	47,58	79,11	259,0	32,42	45,89	241,0	481,3	265,8
5	55,34	91,52	302,7	24,66	33,48	197,3	383,6	163,1
6	60,80	99,98	334,1	19,20	25,02	165,8	308,7	99,33
7	64,7	105,8	357,3	15,31	19,17	142,6	250,1	60,34
8	67,55	109,9	375,1	12,45	15,05	124,9	203,5	36,62
10	71,4	115,1	400,0	8,643	9,865	99,99	135,7	13,48
12	73,69	118,9	416,7	6,314	6,910	83,33	90,78	4,96
15	75,8	120,6	433,3	4,223	4,440	66,67	49,79	1,11
20	77,5	122,5	450,0	2,454	2,500	50,00	18,32	0,09
40	79,4	124,4	475,0	0,625	0,625	25,00	0,34	0,00
$\to\infty$	80,0	125,0	500,0	$10^3/c^2$	$10^3/c^2$	$10^3/c$	$10^3 e^{-0{,}20}$	$\frac{2000}{e^{0{,}5c}}$
	$-10^3/c^2$	$-10^3/c^2$	$-10^3/c$					

Table 3. Values of $10^3 i_{xk}$ for $x_n = 0{,}2\, l_n$

c	End slope	$\frac{k}{l} = 0{,}1$	0,15	0,2	0,3	0,4	0,5	0,6	0,8	End slope
$\to 0$	$9{,}3c^2$	$0{,}87c^2$	$1{,}19c^2$	$1{,}36\,c^2$	$1{,}14c^2$	$0{,}49c^2$	$-0{,}25c^2$	$-0{,}84\,c^2$	$-1{,}04\,c^2$	$6{,}67c^2$
1	9,12	0,854	1,164	1,325	1,111	0,476	− 0,248	− 0,222	− 1,017	6,49
2	34,20	3,204	4,371	4,973	4,141	1,739	− 0,955	− 3,072	− 3,767	24,06
3	69,7	6,53	8,92	10,13	8,36	3,40	− 2,06	− 6,25	− 7,56	48,2
4	109,4	10,28	14,05	15,94	12,93	5.07	− 3,38	− 9,78	−11,65	74,4
5	148,9	14,02	19,11	21,75	17,33	6,49	− 4,84	−13,26	−15,53	99,2
6	185,2	17,49	23,97	27,16	21,25	7,56	− 6,34	−16,43	−18,95	121,1
7	217,1	20,57	28,27	32,03	24,59	8,28	− 7,80	−19,25	−21,83	139,8
8	244,3	23,25	32,05	36,34	27,36	8,71	− 9,15	−21,62	−24,20	155,4
10	285,8	27,46	38,16	43,33	31,49	8,98	−11,49	−25,28	−27,70	179,3
12	313,4	30,44	42,69	48,66	34,20	8,76	−13,34	−27,83	−30,05	196,0
15	336,9	33,32	47,44	54,51	36,66	8,16	−15,31	−30,26	−32,25	213,4
20	351,3	35,71	52,13	60,85	38,58	7,16	−17,22	−32,38	−34,16	230,4
40	344,0	37,19	57,75	71,35	39,64	5,48	−19,32	−34,52	−36,15	255,7
$\to\infty$	320,0	36,80	58,80	83,20	39,20	4,80	−20,00	−35,20	−36,80	280,0
		+980/c²	+990/c²	−500/c +1000/c²	+1010/c²	+1020/c²	+1020/c²	+1020/c²	+1000/c²	

Table 4. Values of $10^3\, i_{xk}$ for $x_n = 0{,}5\, l_n$

c	End slope	$\frac{h}{l} = 0{,}1$	0,2	0,3	0,4	0,5
$\to 0$	$-\ 2{,}60\,c^2$	$-\ 0{,}22\ c^2$	$-\ 0{,}25\ c^2$	$-0{,}04\ c^2$	$0{,}29\ c^2$	$0{,}49\ c^2$
1	− 2,57	− 0,217	− 0,248	−0,045	0,288	0,482
2	− 9,94	− 0,840	− 0,955	−0,170	1,114	1,873
3	− 21,15	− 1,789	− 2,039	−0,363	2,373	4,008
4	− 34,98	− 2,955	− 3,374	−0,623	3,922	6,676
5	− 50,12	− 4,230	− 4,843	−0,932	5,621	9,651
6	− 65,58	− 5,52	− 6,34	−1,42	7,35	12,74
7	− 80,4	− 6,77	− 7,80	−1,63	8,99	15,78
8	− 94,2	− 7,93	− 9,15	−1,99	10,55	18,74
10	−118,1	− 9,90	−11,49	−2,70	13,19	24,06
12	−137,0	−11,45	−13,34	−3,39	15,19	28,50
15	−158,2	−13,10	−15,31	−4,26	17,26	33,80
20	−179,9	−14,73	−17,22	−5,34	19,10	39,92
40	−212,0	−16,72	−19,32	−6,90	20,32	50,54
$\to\infty$	−250,0	−17,50 +1230/c²	−20,00 +1020/c²	−7,50 +870/c²	20,00 +780/c²	62,50 −500/c +750/c²

Table 5. Values of $10^3\, i_{xk}^{\mathrm{I}}$ for $x_n = 0$

c	End slope	$\frac{k}{l}=0{,}05$	0,1	0,2	0,3	0,4	0,5	0,6	0,8	End slope
→0	$125c^2$	$5{,}07c^2$	$8{,}06c^2$	$9{,}33c^2$	$6{,}56c^2$	$2{,}00c^2$	$-\ 2{,}60c^2$	$-\ 6{,}00c^2$	$-\ 6{,}67c^2$	$40{,}7c^2$
1	123,42	4,994	7,920	9,119	6,370	1,908	− 2,576	− 5,868	− 6,496	40,54
2	472,0	19,12	30,10	34,20	23,52	6,68	− 9,94	− 22,00	− 24,06	150,2
3	1014	40,27	62,68	69,67	46,67	12,14	− 21,16	− 44,85	− 48,24	300,7
4	1686	66,0	101,3	109,4	70,9	16,2	− 35,0	− 70,6	− 74,4	463
5	2451	94,2	142,3	148,9	92,7	17,8	− 50,1	− 96,1	− 99,2	617
6	3276	123,6	183,3	185,2	110,6	16,7	− 65,5	−119,8	−121,1	754
7	4142	153,1	222,7	217,1	124,0	13,4	− 80,4	−140,8	−139,8	871
8	5035	182,2	260,0	244,3	133,4	8,5	− 94,2	−158,9	−155,4	970
10	6876	238,2	326,8	285,8	143,1	− 3,5	−118,0	−187,6	−179,2	1125
12	8761	290,4	383,1	313,3	144,8	− 16,0	−137,0	−208,6	−196,0	1239
15	11635	360,9	450,4	337,1	140,4	− 32,6	−157,9	−230,2	−213,1	1365
20	16503	459,1	526,9	351,3	128,6	− 52,6	−179,9	−252,1	−230,4	1497
40	36273	681,4	626,9	344,0	100,8	− 85,3	−214,0	−285,3	−255,7	1726
→∞	$+10^3 c$	807,5 $-10^3\, e^{-0{,}05c}$	630,0 $-10^3\, e^{-0{,}1c}$ + 540/c	320,0 + 960/c	70,0 + 1260/c	−120,0 + 1440/c	−250,0 + 1500/c	−320,0 + 1440/c	−280,0 + 960/c	2000

Table 6. Values of $10^3\, i_{xk}^{\mathrm{II}}$ for $x_n = 0{,}2\, l_n$

c	End slope	$\frac{k}{l}=0{,}1$	0,15	0,2	0,3	0,4	0,5	0,6	0,8	End slope
0	400,0	40,76	62,50	85,76	38,36	0,96	−25,00	−39,04	−34,24	200,0
1	390,4	39,87	61,29	84,39	37,24	0,52	−24,70	−38,18	−33,26	194,0
2	364,0	37,41	57,97	80,66	34,23	−0,61	−23,81	−35,80	−30,60	177,8
3	326,4	33,92	53,24	75,35	30,05	−2,09	−22,47	−32,44	−26,96	155,7
4	284,0	29,98	47,89	69,36	25,48	−3,53	−20,82	−28,68	−23,04	132,2
5	241,5	26,01	42,48	63,36	21,09	−4,70	−19,01	−24,94	−19,36	110,4
6	202,1	22,31	37,47	57,74	17,20	−5,51	−17,15	−21,50	−16,14	91,6
7	167,0	18,99	32,92	52,68	13,89	−5,98	−15,35	−18,45	−13,46	76,1
8	136,7	16,09	28,91	48,19	11,15	−6,17	−13,67	−15,83	−11,27	63,6
10	89,4	11,47	22,40	40,90	7,10	−6,00	−10,76	−11,74	− 8,07	45,5
12	56,8	8,14	17,52	35,32	4,45	−5,46	− 8,49	− 8,87	− 5,97	33,8
15	26,8	4,86	12,40	29,22	2,07	−4,49	− 6,04	− 6,06	− 4,02	23,0
20	4,70	2,03	7,32	22,65	0,28	−3,10	− 3,65	− 3,55	− 2,35	13,62
40	3,25	−0,11	1,22	11,90	−0,56	−0,90	− 0,94	− 0,90	− 0,60	3,59
→∞	$10^3 \cdot 6/c^2$	$-540/c^2$ $+\frac{500}{ce^{0,1c}}$	$-765/c^2$ $+\frac{500}{ce^{0,05c}}$	$500/c$ $-960/c^2$	$-1260/c^2$ $+\frac{500}{ce^{0,1c}}$	$-1440/c^2$	$-1500/c^2$	$-1440/c^2$	$-960/c^2$	$10^3 \cdot 6/c^2$

Table 7. Values of $10^3\, i_{xk}^{II}$ for $x_n = 0{,}5\, l_n$

c	End slope	$\frac{k}{l}=0{,}1$	0,2	0,3	0,4	0,5
0	−125,0	−11,31	−16,00	−8,81	14,00	54,69
1	−122,7	−11,15	−15,82	−8,79	13,77	54,29
2	−117,9	−10,69	−15,25	−8,63	13,14	53,17
3	−110,0	−10,00	−14,39	−8,41	12,18	51,44
4	−100,3	− 9,15	−13,34	−8,12	10,98	49,27
5	− 89,9	− 8,23	−12,18	−7,78	9,68	46,84
6	− 79,4	− 7,31	−10,99	−7,41	8,36	44,30
7	− 69,5	− 6,42	− 9,84	−7,00	7,10	41,78
8	− 60,5	− 5,62	− 8,76	−6,59	5,93	39,35
10	− 45,6	− 4,27	− 6,90	−5,76	3,96	34,92
12	− 34,7	− 3,27	− 5,44	−4,98	2,47	31,14
15	− 23,7	− 2,24	− 3,86	−3,96	0,98	26,60
20	− 13,8	− 1,31	− 2,33	−2,70	−0,24	21,22
40	− 3,59	− 0,34	− 0,60	−0,78	−0,67	11,56
$\to\infty$	$-10^3.6/c^2$	$-540/c^2$	$-960/c^2$	$-1260/c^2$	$-1440/c^2$ $\frac{500}{ce^{0,1c}}$	$500/c$ $-1500/c^2$

Table 8. Values of $10^3\, i_{xk}^{III}$ for $x_n = 0$

$i_{xk}^{III} = 1$ for $k = 0$ and all c

c	End slope	$\frac{k}{l}=0{,}05$	0,1	0,2	0,3	0,4	0,5	0,6	0,8	End slope
0	− 3500	825,6	654,8	336,0	64,8	−144,0	−281,3	−344,0	−264,0	1500
1	− 3626	820,5	646,6	326,6	58,3	−145,7	−278,3	−337,9	−257,8	1462
2	− 3987	806,1	623,8	301,0	41,3	−149,7	−269,9	−321,0	−240,7	1361
3	− 4538	784,2	590,2	264,6	18,2	−153,9	−257,1	−297,0	−217,5	1224
4	− 5228	757,7	550,3	223,7	− 5,9	−156,6	−241,3	−269,8	−192,5	1078
5	− 6011	728,6	507,9	183,1	−27,6	−156,6	−223,9	−242,7	−168,9	943
6	− 6856	698,3	465,4	145,5	−45,3	−153,9	−206,3	−217,4	−148,2	826
7	− 7741	667,9	424,5	112,4	−58,5	−149,0	−189,4	−194,9	−130,7	729
8	− 8654	637,9	385,8	84,1	−67,8	−142,6	−173,5	−175,2	−116,2	649
10	−10531	580,3	316,5	40,6	−77,0	−128,0	−146,1	−143,8	− 94,4	530
12	−12448	526,7	258,1	11,5	−78,2	−113,3	−124,4	−120,8	− 79,1	448
15	−15364	454,4	188,3	−13,8	−73,3	− 94,5	−100,6	− 96,8	− 63,6	364
20	−20277	354,2	108,9	−29,5	−60,7	− 72,1	− 75,5	− 72,5	− 47,8	277
40	−40144	128,3	4,9	−23,6	−31,5	− 36,1	− 37,6	− 36,1	− 24,0	144
$\to\infty$	-10^3c	$10^3e^{-0,05c}$ $-285/c$	$10_3e^{-0,1c}$ $-340/c$	$10^3e^{-0,2c}$ $-960/c$	$-1260/c$	$-1440/c$	$-1500/c$	$-1440/c$	$-960/c$	$10^3.6/c$

Table 9. Values of $10^3\, i_{xk}^{III}$ for $x_n = 0{,}5\, l_n$

c	End slope	$\frac{k}{l} = 0{,}1$	0,2	0,3	0,4	$0{,}5 \pm 0$
0	−1000	−100,0	−200,0	−300,0	−400,0	± 500
1	− 959	− 96,1	−193,2	−292,2	−394,1	± 500
2	− 851	− 85,7	−174,8	−270,9	−377,9	± 500
3	− 704	− 71,4	−149,5	−241,1	−354,5	± 500
4	− 551	− 56,6	−122,4	−208,1	−327,5	± 500
5	− 413	− 43,1	− 97,1	−176,0	−299,7	± 500
6	− 299	− 31,8	− 75,3	−146,8	−272,8	± 500
7	− 212	− 22,9	− 57,6	−121,6	−247,6	± 500
8	− 147	− 16,3	− 43,5	−100,1	−224,4	± 500
10	− 67,4	− 7,9	− 24,4	− 67,5	−183,9	± 500
12	− 29,8	− 3,7	− 13,5	− 45,3	−150,6	± 500
15	− 8,30	− 1,2	− 5,5	− 24,9	−111,6	± 500
20	− 0,91	− 0,2	− 1,2	− 9,2	− 67,7	± 500
40	0	− 0,0	− 0,0	− 0,2	− 9,2	± 500
$\to\infty$	$\frac{10^3 c}{e^{0,5c}}$	$-500e^{-0,4c}$	$-500e^{-0,3c}$	$-500e^{-0,2c}$	$-500e^{-0,1c}$	± 500

Table 10. Values of $10^3\, i_{xk}^{IV}$ for $x_n = 0{,}2\, l_n$

c	End slope	$k = 0{,}1$	0,15	0,2	0,3	0,4	0,5	0,6	0,8	End slope
0	5000	491	719	928	1271	1488	1563	1488	928	−5000
1	5396	531	781	1013	1308	1488	1537	1449	895	−4812
2	6478	642	953	1252	1407	1483	1464	1343	807	−4312
3	7986	800	1202	1610	1547	1465	1354	1192	689	−3648
4	9626	976	1492	2043	1678	1424	1219	1022	565	−2967
5	11158	1150	1792	2520	1797	1360	1073	854	452	−2360
6	12434	1306	2081	3017	1889	1276	926	701	358	−1862
7	13383	1436	2348	3522	1950	1178	787	567	282	−1470
8	13987	1538	2588	4028	1982	1073	660	455	222	−1168
10	14254	1660	2983	5037	1978	863	452	288	140	− 760
12	13551	1690	3271	6037	1907	672	301	181	91	− 497
15	11474	1616	3541	7529	1732	445	159	91	48	− 273
20	7428	1338	3684	10014	1376	210	52	30	18	− 102
40	545	366	2707	20000	367	7	1	0	0	− 2
$\to\infty$	$\frac{10^3 c^2}{e^{0,2c}}$	$\frac{500c}{e^{0,1c}}$	$\frac{500c}{e^{0,05c}}$	$\frac{2 \cdot 10^3}{c}$	$\frac{500c}{e^{0,1c}}$	$\frac{500c}{e^{0,2c}}$	$\frac{500c}{e^{0,3c}}$	$\frac{500c}{e^{0,4c}}$	$\frac{500c}{e^{0,6c}}$	$-\frac{10^3 c^2}{e^{0,8c}}$

Table 11. Values of $10^3\, i_{xk}^{IV}$ for $x_n = 0{,}5\, l_n$

c	End slope	$\frac{k}{l}=0{,}1$	0,2	0,3	0,4	0,5
0	5000	491	928	1271	1488	1563
1	4883	480	913	1262	1501	1616
2	4551	449	896	1136	1539	1772
3	4059	404	802	1194	1593	2019
4	3476	350	720	1040	1656	2341
5	2873	294	632	1075	1720	2719
6	2300	240	543	903	1775	3139
7	1792	191	459	826	1819	3587
8	1364	149	383	647	1847	4054
10	745	86	257	592	1858	5020
12	384	47	167	350	1814	6007
15	130	18	84	175	1675	7502
20	23	3	25	82	1354	10000
40	0	0	0	7	366	20000
$\to\infty$	$\frac{10^3 c^2}{e^{0,5c}}$	$\frac{500c}{e^{0,4c}}$	$\frac{500c}{e^{0,3c}}$	$\frac{500c}{e^{0,2c}}$	$\frac{500c}{e^{0,1c}}$	$10^3 \cdot \frac{1}{2}c$

Table 12. Graphically evaluated positive influence areas A_+ for $i_{xk}^{(i)}$ and simultaneous j_k/g_n-areas H_+ (see note on p. 23).

	$x/l=0{,}2$		0,5		0		0,2		0,5		0		0,5
c	$10^3 A_+$ of i_{xk}	H_+	$10^3 A_+$ of i_{xk}	H_+	$10^3 A_+$ of i_{xk}^{I}	H_+	$10^3 A_+$ of i_{xk}^{II}	H_+	$10^3 A_+$ of i_{xk}^{II}	H_+	$10^3 A_+$ of i_{xk}^{III}	H_+	$10^3 A_+$ of i_{xk}^{III}
0	$0{,}39c^2$	0,445	$0{,}109c^2$	0,552	$1{,}07c^2$	0,407	16,4	0,348	7,28	0,466	151,6	0,242	125,0
1	0,38	0,445	0,107	0,552	1,04	0,407	16,1	0,348	7,20	0,466	149,0	0,240	122,5
2	1,43	0,444	0,418	0,551	3,93	0,405	16,0	0,344	6,93	0,462	142,5	0,231	115,5
3	2,95	0,441	0,90	0,549	8,20	0,402	13,5	0,335	6,56	0,454	134,4	0,218	105,8
4	4,55	0,436	1,48	0,546	12,5	0,395	12,0	0,325	6,12	0,444	124,4	0,205	95,2
5	6,11	0,431	2,11	0,543	16,8	0,385	10,5	0,315	5,63	0,432	114,3	0,189	84,8
6	7,53	0,426	2,73	0,540	21,1	0,376	9,03	0,306	5,12	0,420	105,0	0,174	75,4
7	8,75	0,421	3,34	0,536	24,6	0,368	7,80	0,295	4,64	0,408	96,6	0,159	67,2
8	9,69	0,416	3,95	0,533	27,9	0,360	6,75	0,284	4,22	0,396	89,3	0,146	60,3
10	11,2	0,408	5,05	0,527	33,3	0,345	5,18	0,267	3,46	0,374	77,0	0,125	49,3
12	12,3	0,403	5,85	0,523	37,2	0,332	4,00	0,252	2,87	0,356	67,4	0,109	41,5
15	13,4	0,395	6,78	0,516	41,5	0,320	2,90	0,236	2,15	0,326	56,7	0,089	33,3
20	14,5	0,387	7,70	0,507	45,5	0,307	1,82	0,218	1,45	0,284	44,3	0,068	25,1
40	15,6	0,377	8,60	0,494	52	0,283	0,50	0,147	0,42	0,200	23,9	0,030	12,5
∞	15,9	0,374	9,00	0,488	59	0,359							

Numerical Application to a Three-Span Bridge

The Mount Hope Bridge has three simply supported spans of constant moment of inertia and can thus be analyzed with the tables of the preceding article. Its dimensional and load constants are for the main span: $l_2 = 1188{,}33$ ft., $f_2 = 118{,}795$ ft., $E I_2 = 123{,}511 \cdot 10^9$ ft.^{2} lbs.; for the side spans $l_1 = l_3 = 498{,}33$ ft., $f_1 = f_3 = 20{,}891$ ft., $E I_1 = E I_3 = 120{,}408 \cdot 10^9$ ft.^{2} lbs., sec $\alpha_1 =$ sec $\alpha_3 =$ $= 1{,}0424$; and for the cable $E_c A_c = 29 \cdot 10^6$ lb./in.$^2 \cdot 73{,}92$ in.$^2 = 2140 \cdot 10^6$ lb., elastic length $L_s = 3138$ ft., temperature length $L = \Sigma l_v = 2966$ ft. and coefficient of thermal expansion $\omega = 6{,}5 \cdot 10^{-6}$/deg. F. The dead load of the bridge is $w = w_1 = w_2 = w_3 = 2650$ lb./ft., hence $w_1 l_1 = 1{,}321 \cdot 10^6$ lb., $w_1 l_1^2 = 658 \cdot 10^6$ lb. ft., $w_2 l_2 = 3{,}149 \cdot 10^6$ lb., $w_2 l_2^2 = 3{,}742 \cdot 10^9$ lb. ft. The live load is $p = 750$ lb./ft. If the load correction term in (5) is omitted one finds $P(x)/w = 750/2\,650 =$ $= 0{,}283$. A change in temperature of $t = \pm 60$ deg. F. should be regarded.

The dead load horizontal force figured in either the side span or the main span is found to be $H_w = w_n l_n^2/8 f_n = 1480 w$ ft. $= 3940 \cdot 10^3$ lbs. ($n = 1$ or 2). The proper flexibilities of the spans become by (44) $c_{01} = c_{03} = \sqrt{\frac{3940 \cdot 498^2}{120{,}4 \cdot 10^6}} =$ $= 2{,}85$ and $c_{02} = \sqrt{\frac{3940 \cdot 1188^2}{123{,}5 \cdot 10^6}} = 6{,}71$. The cable factor becomes by (9) $\gamma =$ $= 3940/2{,}14 \cdot 10^6 = 1{,}84 \cdot 10^{-3}$.

To find for example the *maximum moment at* $x_2 = 0{,}2\, l_2$ one may assume tentatively $\beta = 0{,}04$, so that by (44) $c_1 = c_3 = 2{,}9$ and $c_2 = 6{,}9$. Table 1 (or a diagram drawn from it) and (29) gives $G_1 = G_3 = w_1^2 \cdot 498^3 \cdot 0{,}038 = 4{,}68 \cdot 10^6$ w_1^2 ft.^{3}, $G_2 = w_2^2 \cdot 1188^3 \cdot 0{,}0683 = 113{,}6$ $\cdot 10^6$ w_2^2 ft.^{3}, $G = 123 \cdot 10^6$ w^2 ft.^{3}, $G_1/G = 0{,}038$, $G_2/G = 0{,}924$, $G/H_w^2 =$ $123 \cdot 10^6/1480^2 = 56{,}2$ ft.

Now subdivide a unit base (span two), Fig. 2, into ten equal parts. Erect

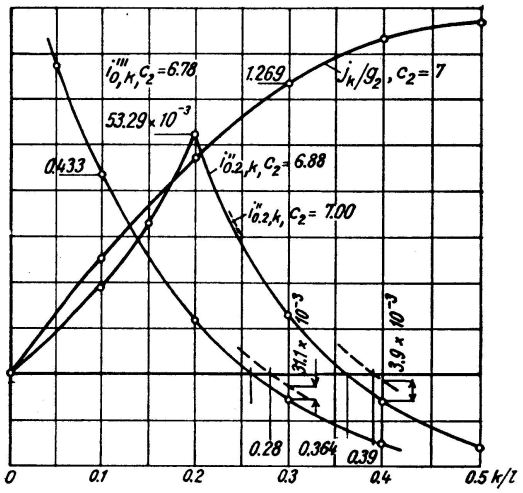

Fig. 2

Note to Table 12

All areas refer to unit span length. The positive area of each influence diagram is denoted by A_+. The negative areas equal the positive areas except for i_{xk} and i_{xk}^{III} at $x = 0{,}5l$ that have two negative areas each equal to $\frac{1}{2}A_+$.

H_+ denotes the area of the j_k/g_n-diagram that is engaged at the same time as the influence lines are loaded on their positive areas A_+. When the negative area(s) of the influence lines is loaded, the corresponding area of the j_k/g_n – diagram is $1 - H_+$.

The total area of the j_k/g_n-diagram is one. The negative areas of the i_{xk}, i_{xk}^{I}, i_{xk}^{II}, and i_{xk}^{III}-diagrams equal the positive areas A_+. The i_{xk}^{IV}-diagram has the positive area one and no negative area. All diagrams i_{xk}^{III} at $x = 0{,}5l$ have $H_+ = 0{,}5$.

according to (31) on these subdivisons the influence ordinates for the span in question, j_k/g_2 for β_2, plotted directly from the nearest figures in Table 1, that is for $c_2 = 7$. Interpolation is seldom necessary at this stage of the investigation. Erect also according to (42) the influence ordinates i_{xk}^{II} for $\frac{M}{w_2 l_2^2}$ at the section $x_2 = 0{,}2\, l_2$ plotted directly from the figures for $c_2 = 7$ in Table 6. According to theorem (43) the correction of i_{xk}^{II} is negative ($T < 1$) in the side spans. Hence the side spans should be left unloaded for maximum positive moment at $x_2 = 0{,}2\, l_2$. When the positive area of the influence line i_{xk}^{II} in span 2 is loaded, the "one-span" horizontal force increment is according) to (31 and Table 12: $\beta_2 = \int \frac{j_k}{g_2 w_2} P(k)\, d\frac{k}{l_2} = \frac{P(k)}{w_2} H_+ = 0{,}283 \cdot 0{,}296 = 83{,}7 \cdot 10^{-3}$ (this figure may also be evaluated by quadrature from Fig. 2).

Equation (32) becomes (load only in the main span) $\beta + \delta = 0{,}924 \cdot 83{,}7 \cdot 10^{-3} = 77{,}4 \cdot 10^{-3}$. For a temperature *rise* of 60 deg. F (23) and (7) give =

$$\delta = \frac{1+\beta}{56 \cdot 2}(\beta \cdot 1{,}84 \cdot 10^{-3} \cdot 3138 + 6{,}5 \cdot 10^{-6} \cdot 60 \cdot 2966)$$

$$\delta = (1 + \beta)\,(102{,}7\,\beta + 20{,}6)\,10^{-3} \qquad (45)$$

Assume (second trial) $\beta = 0{,}050$. This gives $\delta = 27{,}0 \cdot 10^{-3}$ and $\beta = (77{,}4 - 27{,}0)\,10^{-3} = 50{,}4 \cdot 10^{-3}$ and by (44) the incidental flexibilities $c_1 = c_3 = 2{,}85\sqrt{1{,}0504} = 2{,}92$ and $c_2 = 6{,}71\sqrt{1{,}0504} = 6{,}88$.

The influence line i_{xk}^{II} is redrawn for $c = 6{,}88$ in Fig. 2. Its correction according to theorem (43) at $k_2/l_2 = 0{,}4$ is 1,47 times $16 \cdot 10^{-3}\,[1 - (1 - T)\,0{,}924]$ or $3{,}9 \cdot 10^{-3}$, since by (33) $U = \frac{1{,}05}{56{,}2} \cdot 1{,}84 \cdot 10^{-3} \cdot 3138 = 0{,}108$, $T = 0{,}097$. The corrected influence line, used only in determining the critical live load *position*, is indicated by a dashed line in Fig. 2. According to it the live load should be extended to $x_2/l_2 = 0{,}39$. That adds $1{,}43 \cdot 0{,}283 \cdot 0{,}026 = 10{,}5 \cdot 10^{-3}$ to the above value of β_2 and $9{,}7 \cdot 10^{-3}$ to $\beta + \delta$ making $\beta = 27{,}3 \cdot 10^{-3}$ by (45) and $\beta = (77{,}4 + 9{,}7 - 27{,}3)\,10^{-3} = 59{,}8 \cdot 10^{-3}$. The incidental stiffness now becomes $c_2 = 6{,}71\sqrt{1{,}06} = 6{,}91$. This does not noticeably change the horizontal force influence lines nor any other results now obtained.

The extended live load applied to the (uncorrected!) influence line i_{xk}^{II} for $c_2 = 6{,}91$ gives $\int_0^{0{,}39} i_{xk}^{II} \frac{P(k)}{w_2} d\frac{k}{l_2} = 0{,}283\,[7{,}91 \cdot 10^{-3}$ (by Table 12) $- 0{,}026 \cdot 2 \cdot 10^{-3}$ (by Fig. 2)] $= 2{,}224 \cdot 10^{-3}$. Further, by (38), $\delta_2 = \beta_2 - \beta = (83{,}7 + 10{,}5 - 59{,}8)\,10^{-3} = 34{,}4 \cdot 10^{-3}$ and by (42): $M/w_2\, l_2^2 = 2{,}224 \cdot 10^{-3} + 34{,}4 \cdot 10^{-3} \cdot 15{,}7 \cdot 10^{-3} = 2{,}764 \cdot 10^{-3}$, $w_2\, l_2^2 = 3{,}74 \cdot 10^9$ lb. ft., $M = 2{,}764 \cdot 10^{-3} \cdot 3{,}742 \cdot 10^9 = 10{,}34 \cdot 10^6$ lb. ft. This result coincides with the value 10 391 ft. kips figured by STEINMAN [11]). The present analysis discloses that only an unimportant error of $0{,}052/2{,}764 = 1{,}9\,\%$ in M would have entered if no correction

of i_{xk}^{II} had been considered and consequently the load carried only to the zero point of i_{xk}^{II}.

As a second example find the maximum *shear* at the support $x_2 = 0$ of the main span. According to theorem (43) the correction to i_{xk}^{III} ($= 0$) is negative in the side spans, which hence should be left unloaded. When the positive area of i_{xk}^{III} in the main span is loaded, Table 12 indicates that the simultaneous area of the j_k/g-diagram is $H_+ = 0{,}159$ (for $c = 7$). Thus (31) gives $\beta_2 = 0{,}283 \,.\, 0{,}159 = 45{,}0 \,.\, 10^{-3}$, (32) gives $\beta + \delta = 45{,}0 \,.\, 10^{-3} \,.\, 0{,}924 = 41{,}5 \,.\, 10^{-3}$, and (45) still approximately holds, whereby $\beta = 18{,}6 \,.\, 10^{-3}$, $\delta = 22{,}9 \,.\, 10^{-3}$, hence by (44) $c_1 = 2{,}85\sqrt{1{,}02} = 2{,}88$, $c_2 = 6{,}71\sqrt{1{,}02} = 6{,}78$. Expressions (33) give to T about the same value 0,097 as figured in the first example. The correction (10,6) of i_{xk}^{III} at $k_2 = 0{,}3\, l_2$ becomes, see Tables 1 and 2, 1,269 times 0,148 [1 − (1 − T) 0,924] or 31,1 . 10^{-3}. The i_{xk}^{III}-diagram for $c = 6{,}78$ is drawn from Table 8 in Fig. 2. The corrected influence line (dashed) near the zero-point shows that the load should be carried to $k_2 = 0{,}28\, l_2$ for maximum shear. Hence $\int_0^{0{,}28} i_{xk}^{III} \frac{P(k)}{w_2} d\frac{k}{l_2} = 0{,}283[98{,}4 \,.\, 10^{-3}\,(\text{by Table 12}) + 0{,}02 \,.\, 11 \,.\, 10^{-3}\,(\text{by Fig. 2})] =$ $= 27{,}9 \,.\, 10^{-3}$. Equation (38) gives $\delta_2 = \beta_2 - \beta = 26{,}4 \,.\, 10^{-3}$, Table 2 gives $j_{x=0}^{III} = 0{,}148$ and (42) gives $V/w_2 l_2 = 0{,}0279 + 0{,}0264 \,.\, 0{,}148 = 0{,}0318$, $V =$ $= 0{,}0318 \,.\, 3{,}149 \,.\, 10^6 = 10{,}01 \,.\, 10^3$ lbs. If the load had been carried only to the zero-point of i_{xk}^{III} a quite unimportant error $0{,}283 \,.\, 0{,}22 \,.\, 10^{-3}/0{,}0318 = 0{,}20\,\%$ would have entered. The drawing of Fig. 2 and many of the above steps could then have been omitted.

Determine (Example 3) the largest live load suspender pull at the center $x_1 = 0{,}5\, l_1$ of the *side* span! A glance at Table 11 shows that the whole of that span should be loaded. Since j_x^{IV} is negative the corrections (43) to $i_{xk}^{IV} = 0$ in the other two spans are positive. Hence also these spans should be fully loaded, but the effect hereof will be carried to the δ-term according to (42). Equations (31) and (29) give $\beta_1 = \beta_2 = \beta_3 = \frac{P(k)}{w g_\nu} \int_0^1 \frac{w}{w_\nu} j_k\, d\frac{k}{l} = \frac{P(k)}{w} = 0{,}283$. One finds by (32) $\beta = \frac{\Sigma G_\nu}{G}\, 0{,}283 - \delta = 0{,}283 - \delta$, and, roughly using (45) with a minus sign for 20,6 (temperature decrease), $\delta = 9{,}5 \,.\, 10^{-3}$, $\beta = 0{,}274$. (This β marks the highest value of the horizontal force. The cables may be designed by it.) The incidental flexibilities become by (44) $c_1 = c_3 = 2{,}85\sqrt{1{,}274} = 3{,}21$, $c_2 =$ $= 6{,}71\sqrt{1{,}274} = 7{,}57$, which gives, by Table 1 and (29), $G_1 = G_3 = w_1^2 \,.\, 498^3 \,.\, 0{,}042 = 5{,}2 \,.\, 10^6\, w_1^2$ ft.^{3}, $G_2 = w_2^2 \,.\, 1188^3 \,.\, 70{,}5 \,.\, 10^{-3} = 117{,}7 \,.\, 10^6\, w_2^2$ ft.^{3}, $G = 128{,}1 \,.\, 10^6\, w^2$ ft.^{3}, $G/H_w^2 = 58{,}7$ ft. This new value of G shifts δ to $9{,}5 \,.\, 10^{-3} \,.\, 123/128{,}1 = 9{,}1 \,.\, 10^{-3}$, with only negligible changes in c. Equations (33) give $U = \frac{1{,}274}{58{,}7} \,.\, 1{,}84 \,.\, 10^{-3} \,.\, 3138 = 0{,}125$, $T = 0{,}111$, and Theorem (43) and Table 2 yields the correction to i_{xk}^{IV} in span 1: j_k/g_1 times $-0{,}391\,(1 - 0{,}889 \,.\, 5{,}2/128{,}1)$, that is $-0{,}377\, j_k/g_1$. This correction is nowhere larger than i_{xk}^{IV}, see Table 11. Thus the whole of span 1 should remain loaded. Equation (38) furnishes

$\delta_1 = 0{,}283 - 0{,}274 = 0{,}009$. Since the area of the i_{xk}^{IV}-diagram is 1, (42) yields $p_s/w_0 = 1 \,.\, 0{,}283 - 0{,}009 \,.\, 0{,}38 = 0{,}280$. The largest hanger reaction in the side spans thus is $p_s = 0{,}280 \,.\, 2650 = 742$ lbs./ft.

A short investigation shows that the *maximum positive moments in the side span* (Example 4) occur when that side span is fully loaded and other spans unloaded at highest temperature. For $\beta = 0{,}04$, $c_1 = c_3 = 2{,}9$, and $c_2 = 6{,}9$ one finds according to (31) $\beta_1 = 0{,}283 \,.\, 1$ (area of j_k/g-diagram), $\beta_2 = 0$, $\beta_3 = 0$, and by (32) and (45) $\delta = 0{,}038\ \beta_1 - \beta = 10{,}8 \,.\, 10^{-3} - \beta = (20{,}6 + 123{,}3\,\beta)\ 10^{-3}$, dismissing β^2. Thus $\beta = 9{,}8 \,.\, 10^{-3}/1{,}1233 = -\ 9{,}8 \,.\, 10^{-3}$ and by (38) $\delta_1 = 0{,}293$. A refiguring for the actual incidental flexibilities $c_1 = c_3 = 2{,}85\sqrt{0{,}99} = 2{,}84$, $c_2 = 6{,}68$ would change the result unnoticeably. The third equation (42) for $x/l_1 = 0{,}5$ gives $M/w_1 l_1^2 = 0{,}283 \,.\, 0$ (the total area of the i_{xk}^{II}-diagram is zero) + $+\ 0{,}293 \,.\, 57{,}3 \,.\, 10^{-3}$ (for $c_1 = 2{,}84$ by Table 2) $= 16{,}8 \,.\, 10^{-3}$, $M = 16{,}8 \,.\, 10^{-3} \,.\, .\ 658 \,.\, 10^6 = 11{,}1 \,.\, 10^3$ lb. ft.

Numerical Application to a One-Span Bridge

After the numerical application to a three-span bridge has been demonstrated, it may seem superfluous to examplify the simpler case of a one-span bridge. Still, a short example will be given to show at the same time how concentrated loads are treated.

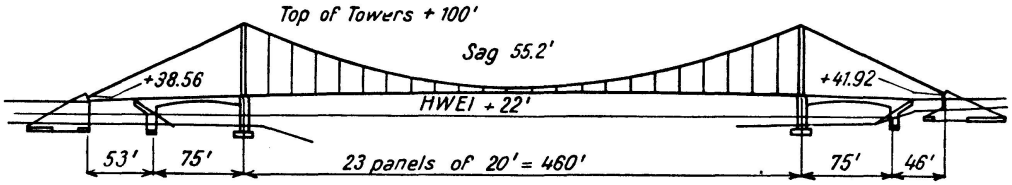

Fig. 3

Fig. 3 shows an elevation of the Boden bridge (Sweden). It has a narrow concrete deck and simply supported steel stiffening girders of uniform stiffness $E I_2 = 4{,}64 \,.\, 10^6$ lb. ft.^{2} (each girder) and dead weight $w_2 = 913$ lb./ft. Its main span is $l_2 = 460$ ft. and the horizontal projections of the free cables in the side spans 249 ft. The cable sag in the main span is $f_2 = 55{,}2$ ft. and the secant of the cable slope in the side spans is sec $\alpha = 1{,}109$. The elastic length of the cable becomes by (11) $L_s = 460\ (1 + 8 \,.\, 55{,}2^2/460^2) + 249 \,.\, 1{,}109^3 = 852$ ft. Its horizontal force is $H_w = w_2 l_2^2/8 f_2 = w_2 l_2/0{,}96 = 438 \,.\, 10^3$ lb., cable area $A_c = 8{,}7$ in.^{2}, $E_c A_c = 247 \,.\, 10^6$ lb., and cable factor (9) $\gamma = 1{,}78 \,.\, 10^{-3}$, $\gamma L_s = 1{,}51$ ft. The proper flexibility by (44) is $c_{20} = \sqrt{H_w l_2^2/EI_2} = 14{,}1$.

Find the critical moment at $x_2 = 0{,}2\, l_2$ caused by a sidewalk load of $p = 126$ lb./ft., $p/w_2 = 0{,}913$, and three concentrated wheel loads of $p\,d\,k = 5500$ lb., $p\,d\,k/w_2 l_2 = 13{,}1 \,.\, 10^{-3}$ each at intervals of 3,94 and 15,7 ft., or in

the unit of the span length 8,6 . 10^{-3} and 36,3 . 10^{-3} (Example 5). If β is roughly estimated at 0,06 the incidental flexibility will be by (44) $c_2 = 14{,}1\ \sqrt{1{,}1} = 14{,}5$. For that value of c plot in Fig. 4 on a unit base the influence lines j_k/g_2 from Table 1, and from Table 6 i^{II}_{xk} for $x/l_2 = 0{,}2$. The latter influence line indicates that the middle wheel load should be placed at $k/l_2 = 0{,}2$. The sidewalk load carried to the zero-point of i^{II}_{xk}, and the wheel load, both applied to the influl ence line j_k/g_2, give the load integra-

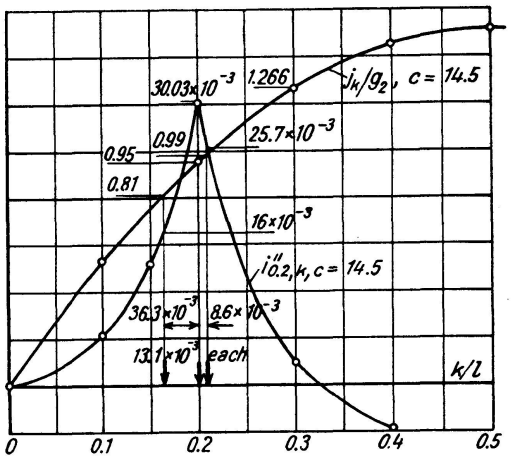

Fig. 4

(31) $\beta_1 = \int \frac{j_k}{g_2}\frac{P(k)}{w_2}\, d\,\frac{k}{l_2} = 0{,}138 \,.\, 0{,}239$ (from Table 12) + 13,1 . 10^{-3} [0,81 + 0,95 + 0,99 (wheel ordinates from Fig. 4)] = 0,0690 = β + δ by (32), since $G_2 = G$. Table 1 and (29) give $G = 0{,}0792\, w_2{}^2 l_2{}^3$, $\frac{G}{H_w^2} = \frac{w^2 l^3 g}{H_w^2} = \left(\frac{wl}{H_w}\right)^2 \lg = \left(\frac{8f}{l}\right)^2 \lg = 0{,}073\, l_2$ = 33,6 ft.; (23) and (7) give $\delta = \frac{1+\beta}{33{,}6\text{ ft.}}\beta \,.\, 1{,}51\text{ ft.} = 0{,}045\ \beta\ (1+\beta)$.

For $\beta = 0{,}65$ one finds $\delta = 3{,}1 \,.\, 10^{-3}$, $\beta = (69{,}0 - 3{,}1)\, 10^{-3} = 65{,}9 \,.\, 10^{-3}$. This corrects the value of the incidental flexibility to $14{,}1\ \sqrt{1{,}0659} = 14{,}6$. The influence lines already drawn in Fig. 4 obviously do not need any redrawing (which, if needed, would be easily effected from the main tables 1 and 6). The influence line i^{II}_{xk} loaded with the same load as for β gives the load integral (42) $\int i^{II}_{xk}\frac{P(k)}{w_2}\, d\,\frac{k}{l_2} = 0{,}138 \,.\, 3{,}05 \,.\, 10^{-3}$ (from Table 12) + 13,1 . 10^{-3} [(16,0 + 30,0 + + 25,7) 10^{-3} (wheel ordinates from Fig. 2)] = 1,36 . 10^{-3}. Table 2 gives j^{II}_x = = 4,50 . 10^{-3}, (38) $\delta_2 = \beta_2 - \beta = \delta = 3{,}1' \,.\, 10^{-3}$, $\delta_2 j^{II}_x = 0{,}014 \,.\, 10^{-3}$, and (42) $M = w_2\, l_2{}^2 \,.\, 1{,}374 \,.\, 10^{-3} = 266 \,.\, 10^3$ lb. ft.

Continuous Stiffening Girders

For continuous bridges it is evidently posssible to evaluate tables of influence functions which are parallel to those here given for simply supported spans.[31]) All bridges with the same span length ratios and the same relative stiffness variation may be covered with one set of such tables.

However, bridges with continuous girders of constant stiffness in each span may be treated with the sole aid of the previous tables. For that purpose the influence of an applied moment M_a to the stiffening girder, notably at its supports, shall be considered. Since the internal work of shear is neglected,

---

[31]) Such influence functions may also be evaluated by model tests[18]).

such a moment may be replaced by two vertical forces $-\frac{M_a}{\Delta k}$ and $+\frac{M_a}{\Delta k}$ on a distance Δk near the point of application of the moment, making Δk tend to zero. *These two forces applied to any influence line* $I_{xk}^{(i)}$ *add*

$$-\frac{M_a}{\Delta k} I_{xk}^{(i)} + \frac{M_a}{\Delta k}\left(I_{xk}^{(i)} + \frac{\partial I_{xk}^{(i)}}{\partial k}\Delta k\right) = M_a \frac{\partial I_{xk}^{(i)}}{\partial k}$$

to the load integral $\int I_{xk}^{(i)} P(k)\, dk$ (46)

The moment M_a is counted positive when turning in a positive direction (from that of x to y). To the right end of the $(n-1)$st span apply a moment $-M_T$ and to the left end of the nth span apply the opposite moment M_T. Both these moments cause tension in the bottom of the stiffening girder. At a continuous support the tower moments M_T must be so chosen that the grades η' on either side of the support become equal. Applying such conditions the unknown tower moments may be solved from a linear system of equations. This method may be used in the determination of individual statical quantities (η, η', M, V, or p_s) and also in the computation of influence functions.

Numerical Application to a Continuous Bridge

Determine the tower moments M_2 and M_3 of the Mount Hope bridge if it were continuous, for a live load extending from $k/l_1 = 0$ to $k/l_2 = 0{,}35$ (Example 6). If, tentatively, $\beta = 0{,}6$, (44) gives $c_1 = c_3 = 2{,}94$, $c_2 = 6{,}91$. In Fig. 5 the influence diagrams j_k/g_2 and i_{xk}^{I} for $x_2 = 0$ and l_2 are plotted from the tables 1 and 5.

By (31) and Theorem (46) is obtained $\beta_1 = \frac{P(k)}{w_1} \cdot 1 + \Sigma \frac{\partial j_k/g_1}{\partial k/l_1}\frac{M}{w_1 l_1^2} =$ $0{,}283 + -\,5{,}047 \cdot 10^{-3}$, (for $c = 2{,}94$ by Table 1) $(-\frac{M_2}{w_1 l_1^2}) = 0{,}283 + 7{,}67\, m_2$, abbreviating $10^{-12}\, M_T/\text{ft. lb.} = m_T$, $M_T/w_1 l_1^2 = 1520\, m_T$, $M_T/w_2 l_2^2 = 267\, m_T$, $\beta_2 = 0{,}283 \cdot 0{,}35 \cdot 0{,}793$ (that is the average height from Fig. 5 of loaded part of the j_k/g_2-diagram) $+ 5{,}195 \cdot 10^{-3}$ (for $c = 6{,}91$ by Table 1) $\left[\frac{M_2}{w_2 l_2^2} - \left(-\frac{M_3}{w_2 l_2^2}\right)\right] = 78{,}5 \cdot 10^{-3} + 1{,}39\,(m_2 + m_3)$, $\beta_3 = 0 \cdot 1 + 5{,}047 \cdot 10^{-3}\frac{M_3}{w_3 l_3^2} = 7{,}67\, m_3$, so that by (32) = and the values of G_ν/G used for the simple span bridge $\delta = 0{,}038\,(\beta_1 + \beta_3) + 0{,}924\beta_2 - \beta = 83{,}3 \cdot 10^{-3} + 1{,}58\,(m_2 + m_3) - \beta = (20{,}6 + 123{,}3\beta + 103\,\beta^2)\, 10^{-3}$, the last member being substituted from (45), $\beta = 55{,}5 \cdot 10^{-3} + 1{,}40\,(m_2 + m_3)$.

Hence by (38) $\delta_1 = \beta_1 - \beta = 227{,}5 \cdot 10^{-3} + 6{,}27\, m_2 - 1{,}40\, m_3$, $\delta_2 = 23{,}0 \cdot 10^{-3} - 0{,}01\,(m_2 + m_3)$, $\delta_3 = -\,55{,}1 \cdot 10^{-3} - 1{,}40\, m_2 + 6{,}27\, m_3$.

Equating the change of grade on either sides of the left tower, the second equation (42) multiplied by $H_w(1+\beta)$ yields $1{,}321 \cdot 10^6$ [0,283 . 0 (total area of i^{I}_{xk}-diagram is zero) + 0,982 (from Table 5) . $(-M_2/w_1 l_1^2)$ + $(227{,}5 \cdot 10^{-3} + 6{,}27\, m_2 - 1{,}40\, m_3)$ (−0,194, from Table 2) = $3{,}149 \cdot 10^6$ [0,283 . 0,35 . 0,168 (average height from Fig. 5 of loaded area of i^{I}_{xk} for $x = 0$) + 4,064 (from Table 5) . $M_2/w_2 l_2^2$ + 0,860 $(-M_3/w_2 l_2^2)$ + $(23{,}0 \cdot 10^{-3} - 0{,}01\, m_2 - 0{,}01\, m_3)$ . . 0,355 (from Table 2)]. Hence $-1493\, m_2 - 44{,}1 \cdot 10^{-3} - 1{,}2\, m_2 + 0{,}3\, m_3 = 2{,}384\,(16{,}6 \cdot 10^{-3} + 1085\, m_2 - 230\, m_3 + 8{,}2 \cdot 10^{-3})$ or $4081\, m_2 - 549\, m_3 = -103{,}2 \cdot 10^{-3}$.

The same steps for the right tower are $3{,}149 \cdot 10^6$. [0,283 . 0,35 . 0,109 + + 0,860 $M_2/w_2 l_2^2$ + 4,064 $(-M_3/w_2 l_2^2)$ + $23{,}0 \cdot 10^{-3}$. 0,355] = $1{,}321 \cdot 10^6$ [0,982 $M_3/w_3 l_3^2$ + $(-55{,}1 \cdot 10^{-3} - 1{,}40\, m_2 + 6{,}27\, m_3)$ 0,194], or $-549\, m_2 + 4081\, m_3 = +56{,}0 \cdot 10^{-3}$. The solution of these two equations is $M_2 = 23{,}9 \cdot 10^6$ ft. lb., $M_3 = 10{,}5 \cdot 10^6$ ft. lb.

These calculations can be considerably shortened if one observes that the tower moments have a negligible influence upon β_ν, β, and δ_ν. Then they read $\beta_1 = 0{,}283$, $\beta_2 = 0{,}283 \cdot 0{,}35 \cdot 0{,}793 = 78{,}5 \cdot 10^{-3}$, $\beta_3 = 0$, $\delta = 0{,}038 \cdot 0{,}283 + 0{,}924 \cdot 0{,}0785 - \beta = 83{,}3 \cdot 10^{-3} - \beta = (20{,}6 + 123{,}3\,\beta)\, 10^{-3}$, $\beta = 55{,}8 \cdot 10^{-3}$, $\delta_1 = 227{,}2 \cdot 10^{-3}$, $\delta_2 = 22{,}7 \cdot 10^{-3}$, $\delta_3 = -55{,}8 \cdot 10^{-3}$, $1{,}321 \cdot 10^6$ [0,982 $(-M_2/w_1 l_1^2)$ + $227{,}2 \cdot 10^{-3}$ (−0,194)] = $3{,}149 \cdot 10^6$ [0,283 . 0,35 . 0,168 + 4,064 $M_2/w_2 l_2^2$ + 0,860 $(-M_3/w_2 l_2^2)$ + $22{,}7 \cdot 10^{-3}$. 0,355], $-1493\, m_2 - 44{,}1 \cdot 10^{-3} = 2{,}384\,(16{,}6 \cdot 10^{-3} + 1085\, m_2 - 230\, m_3 + 8{,}1 \cdot 10^{-3})$, $4080\, m_2 - 548\, m_3 = -103{,}0$, $3{,}149 \cdot 10^6$ [0,283 . 0,35 . 0,109 + 0,860 $M_2/w_2 l_2^2$ + 4,064 $(-M_3/w_2 l_2^2)$ + $22{,}7 \cdot 10^{-3}$. 0,355] = $1{,}321 \cdot 10^6$ [0,982 $M_3/w_3 l_3^2$ − 55,8 . 0,194), $-548\, m_2 + 4080\, m_3 = 55{,}9 \cdot 10^{-3}$, with the same solution M_2, M_3 as above.

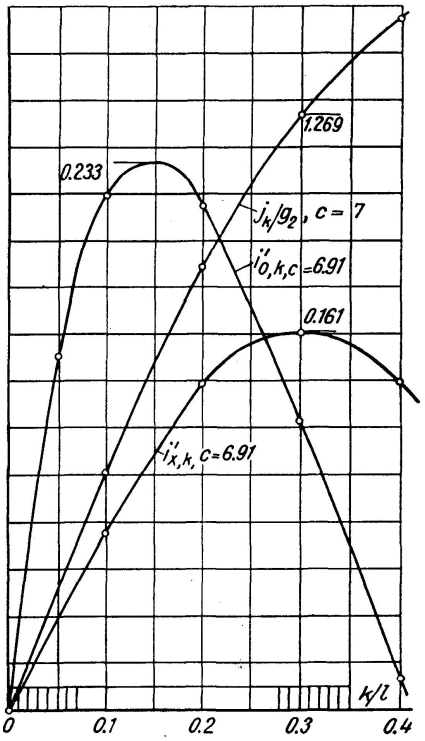

Fig. 5

On account of the large bending moments a local increase in the strength and stiffness of the truss at the towers is economically justified. A local increase in stiffness does not need to change the stress distribution very much, but to be exact other sets of influence tables for varying stiffnesses could be computed, departing from (16), and used together with all formulas here given before (43). Such influence tables may also be accurately determined by model methods [18]).

In a complete analysis of a continuous bridge with even stiffness in each span, influence lines may be computed from the above tables or from a more complete set of tables for even stiffness. The influence diagram for a tower moment is, for instance, obtained by severing the girder at the tower and

applying an external tower moment M_T of such a magnitude that the difference in change in grade on both sides of the tower equals one, Then the deflection of the truss becomes an influence diagram for the tower moment. This diagram is to be determined for several values of the incident flexibility that may arise.

APPENDIX

Notation

All notation except that which is specific to this paper, is in conformance with common usage in most American treatises on the theory of suspension bridges. References to the numbered equation where the magnitude is first defined or used is given within parentheses. Refer also to Fig. 6.

A_c = section area of cable, A_{c0} = a mean value of A_c (10), A_+ = positive area of influence diagram

C = cable, ΔC = cable yield (7)

c_n = incidental flexibility of span n (44)

c_{0n} = proper flexibility of span n (44)

E, E_c = modulus of elasticity of truss and cable (5), e_{xk} = distinct unity ordinate at $x = k$ (25)

f_ν = vertical cable sag measured from the cable cord at the center of the νth span (11)

G = bridge constant (22), G_ν = contribution to G from the νth span (29), g_ν = span constant in one-span bridge (29)

H_w = horizontal force of dead load $= -y''/w$, H = increment of horizontal force due to other causes, H_+ = area of the j_k/g-diagram engaged at the same time as another influence diagram is loaded on its positive area A_+.

I = moment of inertia of truss at section x (5), I_ν = constant value of I in the νth span (44).

I_{xk}, I^{I}_{xk}, etc. = working influence functions (25), $i^{(i)}_{xk}$ = working influence functions for one-span bridge (41)

J_{xk}, J_x, j_{xk}, j_x, J^{I}_{xk}, etc. = influence functions (19) (21) (25) (27) (28)

k = abscissa of live load elements, $K = k/l_n$ (27)

L = horizontal distance between cable anchorages (7), ΔL = increase of L due to anchorage displacement (7), L_s = "elastic length" of cable (10), l_ν = = length of νth span.

M = moment in stiffening truss at section x (14), M_1 and M_2 = particular solutions of homogeneous equation (16), M_a = external moment applied to the stiffening girder, M_T = tower moment in continuous girder.

m = span not containing the section x (37), also subscript.

N = total number of spans.

n = span containing the section x (18), also subscript.

$P(k)$ = load function (5), p, $p(k)$ = distributed live load at abscissa k (5), $p_t(x)$ = live load carried by the stiffening truss (5), $p_s(x)$ = live load carried by the suspenders (3).

s = length of dead load cable arc measured from left support or saddle to section x (1).

t = uniform *rise* in temperature (7), temporarily used abscissa (18).

T, U = quantities used in ascertaining the critical live load position (33).

V = shear in stiffening truss at section x (26).

$w(x)$ = variable dead load per unit of length of bridge (3), w_n = a mean value of w in the nth span (28).

x = abscissa measured from the left support of the nth span to the section to be investigated, $X = x/l_n$ (27).

y = ordinate measured downwards from a horizontal line to the cable under dead load at section x.

α_ν = slope of cable chord in the νth span (11).

$\beta = H/H_w$ relative increment of horizontal force (8), $\beta_\nu = \beta$ in one-span bridge with inextensible cables (31).

γ = cable factor (9).

δ = cable yield constant (23), δ_0 = same for corrected equations (34), δ_n = same including all span interaction effects (38), see also (42).

ϵ = elastic and temperature unit elongation of cable.

η = vertical displacement of truss at section x due to live load, temperature, and anchorage displacement.

ξ = horizontal displacement of the cable point originally at abscissa x due to same causes.

Φ = load function (5).

ψ = direction of tangent of deformed cable (2).

ω = coefficient of thermal expansion (7).

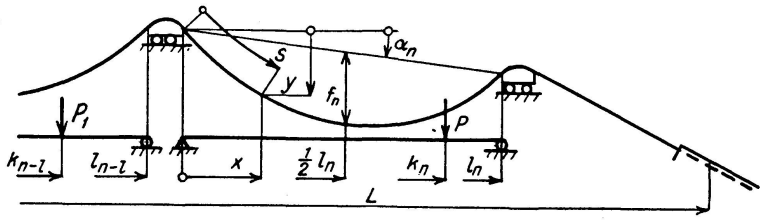

Fig. 6

Summary

A general, systematic influence line method for the analysis of variable stiffness suspension bridges is deduced. Here minor effects, such as caused by cable extension, span interaction, and angular deviations, are segregated to simple correction terms. This makes possible the treatment by large classes, of bridges

containing spans of arbitrary stiffness variations and arbitrary cable arrangements. In this treatment *direct* use is made of tabulated influence functions for inextensible cable, *simple* span bridges of the same stiffness variations as contained in the bridge to be analyzed.

Such influence functions for *uniform* stiffness spans are tabulated in the paper. Constraint values are also tabulated, by which continuous bridges may be treated according to methods deduced in the paper. Numerical examples are elaborated with very complete cross-references, so as to make feasible, without an absolute insight in the underlying theory, the practical computations of one-span and multiple-span bridges. Practical examples solved should serve as an incitement and a port of entry for gradually extended investigations in the theoretical parts of the paper.

Zusammenfassung

Eine allgemeine, systematische Methode zur Berechnung von Versteifungsträgern variabler Steifigkeit mit Hilfe von Einflußlinien wird abgeleitet. Kleinere Einflüsse, hervorgerufen durch die Kabeldehnung, das Zusammenwirken der verschiedenen Felder und die Kabelkrümmung, werden ausgeschieden und zu einfachen Korrekturgliedern zusammengefaßt. Dies ermöglicht die gruppenweise Behandlung der verschiedensten Typen von Hängebrücken mit Versteifungsträgern beliebig veränderlicher Steifigkeit und beliebiger Kabelanordnung. In dieser Berechnung werden tabulierte Einflußfunktionen für starre Kabel *direkt* gebraucht für *einfeldrige* Brücken mit den gleichen Streifigkeitsverhältnissen, wie sie die zu untersuchende Brücke aufweist.

Solche Einflußfunktionen für Felder mit konstanter Steifigkeit sind im Beitrag zusammengestellt. Auch für die Formänderungswerte werden Tabellen gegeben; damit können durchlaufende Versteifungsträger mit der gleichen, im Beitrag entwickelten Methode berechnet werden.

Numerische Beispiele werden durchgearbeitet und ausführlich erklärt, um die praktische Berechnung von ein- und mehrfeldrigen Brücken so darzustellen, daß ein in das Detail gehendes Studium der zu Grunde liegenden Theorie nicht nötig ist. Die gelösten praktischen Beispiele dienen als Anregung und Einführung zum eingehenderen Studium der im vorliegenden Beitrag entwickelten Theorien.

Résumé

L'auteur établit une méthode générale, systématique, pour le calcul des poutres raidisseuses de rigidité variable, à l'aide de lignes d'influence. Il considère séparement les influences secondaires dues à la dilatation des câbles, à l'interaction des différentes travées et à la courbure des câbles, en les groupant

sous la forme de termes simples de correction. Cette méthode permet d'étudier, en les classant par groupes, les types les plus divers de ponts suspendus, avec poutres raidisseuses de rigidité variable et dispositions arbitraires pour les câbles.

Dans ce calcul, l'auteur utilise *directement* les fonctions d'influence présentées sous forme de tableaux, pour câbles rigides, en les appliquant à des *ponts à une seule travée* accusant les mêmes conditions de rigidité que le pont à étudier lui-même.

L'auteur expose dans sa communication des fonctions d'influence de cet ordre, s'appliquant à des travées de rigidité constante. Il donne également des tableaux pour les valeurs des déformations. Il est ainsi possible de procéder au calcul des poutres raidisseuses continues à l'aide de la même méthode.

Des exemples numériques sont exposés d'une manière détaillée; ils mettent en lumière le mode de calcul pratique des ponts à une et à plusieurs travées, dans des conditions telles qu'il devient inutile d'étudier d'une manière approfondie la théorie de base. Les exemples pratiques ainsi résolus n'en incitent pas moins le lecteur à pousser plus loin l'étude des théories exposées dans ce mémoire.

Leere Seite
Blank page
Page vide